UNIVERSIDAD DE CHILE
FACULTAD DE CIENCIAS FÍSICAS Y MATEMÁTICAS
DEPARTAMENTO DE INGENIERÍA MECÁNICA

# CHARACTERIZATION OF COPPER SLAG FOR THERMAL ENERGY STORAGE

MEMORIA PARA OPTAR AL TÍTULO DE INGENIERA CIVIL MECÁNICA

VALENTINA CONSTANZA SEGOVIA ARAYA

PROFESOR GUÍA:
JOSÉ MIGUEL CARDEMIL IGLESIAS

MIEMBROS DE LA COMISIÓN:
RUBÉN FERNÁNDEZ URRUTIA
DIEGO VASCO CALLE

SANTIAGO DE CHILE
2020

RESUMEN DE LA MEMORIA PARA OPTAR
AL TÍTULO DE INGENIERA CIVIL MECÁNICA
POR: VALENTINA CONSTANZA SEGOVIA ARAYA
FECHA: ENERO 2020
PROF. GUÍA: JOSÉ MIGUEL CARDEMIL IGLESIAS

# CHARACTERIZATION OF COPPER SLAG FOR THERMAL ENERGY STORAGE

Due to the increasing energy demand predicted for the following 30 years, the integration of renewable energy to the global energy grid, is considered one of the most important strategies to fight climate change. Since solar energy is one of the largest energy sources available, the development and improvement of solar technologies is a key point for this purpose, especially for solar thermal technologies. Establishing high temperature thermal storage systems makes it possible to develop higher concentrated solar power (CSP) generation. By storing heat in a material at high temperatures, a power block (usually a steam turbine) can be connected to the storage system, allowing the supply of energy regardless of the solar resource. Several authors have characterized by-products and recycled materials from different industries, to be used as filler material for packed-bed thermal energy storage (TES) systems, due to their low cost and high thermo-physical properties; instead of commonly used molten salts, which, despite having a high thermal capacity, their limited operating temperature range, especially their high freezing points, and costs associated with acquisition and maintenance of the system, present major obstacles to the development of CSP technologies. Therefore, different alternatives are being studied, especially industrial by-products, due to their low cost and high availability. A potential alternative for high temperature thermal storage is copper slag. This material is composed mainly of ferrous elements, which offer potential thermo-physical properties, especially since it is a by-product of a high temperature process (melting point near 1300°C). In the present work, an experimental approach for the characterization of copper slag is carried out, with the objective of evaluating the thermo-physical properties of copper slag, specifically: thermal stability, specific heat, thermal conductivity and density. Through thermal gravimetric analysis, it was possible to determine the thermal stability of copper slag after being thermally treated three times up to 800°C. The DSC analysis concluded that copper slag has high $Cp$ values, from 1.4 to 2.1 $[J/gK]$, in a temperature range from 100°C to 500°C, with unstable behavior and reactive to certain temperature points, for samples that were not previously thermally stabilized. However, a $Cp$ curve with linear behavior from 0.8 to 1.1 $[J/gK]$, was obtained, on a test from room temperature to 450°C, for a thermally stabilized sample, which is consistent to literature. These results are relatively high compared to conventional materials and materials from literature. The KD2 Pro device results presented a consistent reverse relation between porosity and thermal conductivity, however the amount of results were not enough to determine thermal conductivity of a full size slag sample. Average Density results were 3456 $[kg/m^3]$ to 3715 $[kg/m^3]$, which in addition to $Cp$ results, imply an overall high thermal capacity for copper slag. However, results and analysis at higher temperatures were not possible to obtain, being a large part of the interest of the characterization of copper slag. It is presented as future work, to complement the characterization with experimental analyses in a range of temperature greater than 600°C.

RESUMEN DE LA MEMORIA PARA OPTAR
AL TÍTULO DE INGENIERA CIVIL MECÁNICA
POR: VALENTINA CONSTANZA SEGOVIA ARAYA
FECHA: DICIEMBRE 2020
PROF. GUÍA: JOSÉ MIGUEL CARDEMIL IGLESIAS

# CARACTERIZACIÓN DE ESCORIA DE COBRE PARA SISTEMAS DE ALMACENAMIENTO TÉRMICO

Debido a la creciente demanda energética prevista para los próximos 30 años, la integración de las energías renovables en la red energética mundial, se considera una de las estrategias más importantes para combatir el cambio climático. Dado que la energía solar es una de las fuentes de energía más grandes disponibles, el desarrollo y la mejora de las tecnologías solares es un punto clave, especialmente para tecnologías termosolares. Establecer sistemas de almacenamiento térmico de altas temperaturas, posibilita el desarrollo de sistemas de concentración solar de alta potencia (CSP). Al almacenar calor a latas temperaturas en un material, se puede conectar un bloque de potencia (generalmente una turbina de vapor) al sistema de almacenamiento, permitiendo el suministro de energía independiente del recurso solar en el momento. Varios autores han caracterizado subproductos y materiales reciclados de diferentes industrias, con potenciales propiedades termo-físicas para ser utilizados como material de relleno para sistemas de almacenamiento térmico packed-bed, debido a su bajo costo y propiedades termo-físicas altas; en vez de la utilización de sales fundidas, las cuales, a pesar de tener una alta capacidad térmica, su limitado rango de temperaturas de operación, especialmente sus altos puntos de congelación, y costos asociados a adquisición y al mantenimiento del sistema, presentan obstáculos importantes para el desarrollo de tecnologías CSP. Por ello, se están estudiando diferentes alternativas, especialmente los subproductos industriales, debido a su bajo costo y gran disponibilidad. Una alternativa potencial para el almacenamiento térmico a alta temperatura es la escoria de cobre. Este material está compuesto principalmente de elementos ferrosos, que ofrecen potenciales propiedades termo-físicas, especialmente debido a que es un subproducto de un proceso de alta temperatura (punto de fusión a los 1300°C). En este trabajo se presenta un enfoque experimental para la caracterización de escoria de cobre, con el objetivo de evaluar las propiedades termo-físicas de la escoria de cobre, específicamente: estabilidad térmica, calor específico, conductividad térmica y densidad. Mediante análisis de gravimetría, fue posible determinar la estabilidad térmica de la escoria de cobre luego de ser tratada térmicamente tres veces hasta 800°C. El análisis DSC concluyó que la escoria de cobre tiene un alto valor de $Cp$, de 1.4 a 2.1 $[J/gK]$ en un rango de temperatura de 100 a 500°C, con comportamientos inestables y reactivos con la temperatura, para muestras que no fueron previamente térmicamente estabilizadas. Sin embargo, se obtiene una curva de $Cp$ con comportamiento lineal, de 0.8 a 1.1 $[J/gK]$, desde temperatura ambiente a 450°C, para una muestra estabilizadas térmicamente, siendo consistente con la literatura. Estos resultados son relativamente altos en comparación a materiales convencionales y materiales en estudio. Los resultados de densidad presentaron un promedio de 3456 $[kg/m^3]$ a 3715 $[kg/m^3]$, que junto con los resultados de $Cp$, implican una alta capacidad térmica para la escoria de cobre. Sin embargo, resultados y análisis a temperaturas mayores no fueron posibles de obtener, siendo gran parte del interés de la caracterización de escoria de cobre. Se presenta como trabajo a futuro, complementar la caracterización con análisis experimentales en un rango de temperatura mayor a los 600°C.

*"A picture with*
*a smile – and*
*perhaps, a tear."*

# Acknowledgment

En primer lugar, quisiera agradecer a mis profesores miembros de esta comisión. Al profesor Rubén Fernández, por tener siempre la disposición a ayudar en lo que pudiera, respecto a la metodología experimental de esta memoria, pero también, por ser un excelente docente que intenta que sus alumnos se cuestionen la razón de las cosas. A mi profesor guía José Miguel Cardemil, por no solo ser un excelente docente y mentor, permitiendo la oportunidad de redescubrir mis deseos de trabajar en investigación, sino que por su comprensión y por el hecho de ser simplemente humano, entregándome atención, tiempo y espacio en los momentos personalmente difíciles de este año, que dificultaron mi trabajo y rendimiento. Por todo esto, estoy profundamente agradecida.

A mis amigos y compañeros que hice durante estos últimos 7 años. Al Team Ñoñef, por ser un grupo de personas increíblemente buenas que se formó en plan común. Los paseos, las risas en clases con las niñas, las tarde enteras en la pajarera; todo esos lindos recuerdos no me los quita nadie. Gracias por hacer los años de plan común tan amigables, a esa provinciana que llegó a Santiago sin conocer nada ni nadie. A la gente de mecánica, tanto alfas como betas; al Tente por hacerme reír y rabiar desde el primer año. A la Noe y Nacha, por el apoyo moral y emocional hasta la fecha. A la Nati y Yani, por los tiempos que compartimos en el Eolian y las oncecitas. A la Fran, por enseñarme a crecer, por escucharme y permitirme escucharla, sin juzgar y apoyándonos la una a la otra, con una dona y un café.

A mis queridas amigas del colegio Cami y Sofi. No se que hubiese sido de mi sin ustedes todos estos años en Santiago. Fueron mi apoyo cuando más débil y deprimida estuve, y pesar de lo mucho que las hice rabiar de vez en cuando, siempre estuvieron para darme un abrazo y palabras de apoyo cuando lo necesitaba. Estar lejos de la familia desde los 18 años no es tan fácil como suena, pero sé que pudimos lograrlo siendo un apoyo la una para la otra, compartiendo y creciendo juntas estos años, y los que vendrán.

Finalmente, quiero darle las gracias a mi familia. A mi mamá que me permitió vivir y estudiar en Santiago cuando decidí que quería estudiar ingeniería. Te esforzaste hasta el cansancio para ayudarme a cumplir mis sueños, preguntándome siempre si estaba contenta, si estaba cansada, si era muy difícil. Tu preocupación fueron bencina para superar cada semestre. A mi papá, por aconsejarme cuando me sentía cansada, ayudándome a entender que a veces es necesario bajar los brazos para tener más energía en el siguiente round. Por velar que nunca me faltara nada, especialmente para comer. Por hacerme rabiar y reír como un padre que nunca dejó de ser niño. A mi familia Segovia y Araya, por ser una familia gigante con personas que me han enseñado, que me han cuidado y apoyado estos años. A mis primos Segovia por hacerme reir y ayudarme con los salvavidas (gracias Jorge y Papia), a mis primitas Araya que me ayudaron a mantener siempre mi infantilidad. Y especialmente a la persona más admirable que podría haber tenido la fortuna de tener en mi vida, como mi tía, como mi segunda mamá. Tía Picha, hubiese deseado darle las gracias en persona. Me cuidó incluso antes de si quiera tener conciencia de la vida, me enseñó a valorar lo simple, a encontrar lo bueno dentro de todo lo malo, me entendió como hija y mujer, me regaloneó siempre y se preocupó de mi, a su manera tan genial y sensata. Gracias por los mejores consejos de vida, y escapes espontáneos de la vida misma. Hasta pronto.

# Table of Contents

# List of Tables

# List of Figures

# Chapter 1

# Introduction

Energy storage technologies are one of the principal issues to consider on a energy supply system. Depending on the physics of the energy source, different energy storage methods and technologies can be implemented. For instance; solar photovoltaics (PV) systems are commonly coupled to batteries due to the photoelectric effect of cells; whilst in the case of dams from hydroelectric plants, energy storage is based on the gravitational potential energy of the reservoir. Thereby, it is clear that for concentrated solar power (CSP) technologies, the storage media demands to store thermal energy efficiently, as it is the way to make up for the solar source variability. Thus, CSP plants are equipped with thermal energy storage (TES) systems, in order to provide heat in a dispatchable way to a power block (commonly a steam turbine), giving operation flexibility even during periods of low solar radiation.

TES technologies for CSP consists of storing a material, liquid or solid, that is able to capture and release thermal energy upon when needed. The chosen material is stored in a type of tank or accumulator to preserve heat, and can either transfer heat itself throughout a heat exchanger, or by using a heat transfer fluid (HTF) on a separated circuit. In general, CSP plants use molten salt mixtures as HTF and heat sensible material for storage, due to its high thermal capacity. However, using molten salts has several techno-economical disadvantages. For instance, its operation temperature range is restricted by a high freezing temperature point, between 120 and 260°C [1, 2], which presents a risk for CSP system performance, allocated in deserted regions where nights have low temperatures that can cause relevant heat losses. Furthermore, molten salts boiling point is around 565°C, which is a limitation for new generation of CSP technologies, in the range of 300 to 800°C, or even higher [2, 3]. Additionally, high costs related to procurement of molten salts and materials to prevent corrosion in conduction systems and valves, plus the complex heat exchanger systems, to make up for molten salts low thermal conductivity, translate into a high cost of deployment for the TES system only. These disadvantages encourage the seek of other alternatives of sensible heat materials for the development of new cost-effective solutions.

Packed-bed storage technologies utilize filler materials to preserve and improve the thermal stratification within the HTF of the storage tank. The transition area between the hot and cold zones, is called thermocline, which allows to store in the same tank thermal energy for charging and discharging of heat. Moreover, packed-bed storage models have shown a

high performance on heat storage capability, with a desirable and effective cost reduction, due to a single tank implementation rather than a two tank storage system for molten salts [4]. This type of heat storage consists basically on a single tank with two filler mediums: a solid sensible heat material and a HTF. The selection of these materials require a number of properties such as; high thermo-physical properties, like specific heat capacity, thermal conductivity and density; chemical properties, as non-reactivity amongst the mediums and throughout the several heating cycles; economic properties, as low cost and availability. With this approach, different authors have suggested the implementation of industrial by-products, such as residues from the iron and steel-making process, which are produced in large scale, allowing their utilization for several applications. These type of by-products, have shown high stability and heat storage capacity in a packed bed configuration (using air as HTF), proving to be an efficient alternative for TES systems [4].

Copper slag from the mining industry has come across as a possible alternative with high potential thermal properties, since it is composed primarily by ferrous components, and is a by-product of a process under high thermal conditions. Thus far, copper slag has been characterized in order to be compared in the selection of recycled materials for high temperature TES, in the case study by Navarro et al. [5], where different mortar formulations of copper slag were characterized and analyzed. The results on this study are a first approach on its characterization and potential properties, however can not be generalized and implemented on a practical model of a packed-bed storage system; specially since copper slag is highly heterogeneous, and its specific composition can vary depending on the minerals of the ore deposit, or the components concentration resulting from the ore leaching process. Therefore, the present work aims to characterize copper slag's thermal capacity by analyzing its specific heat capacity, thermal conductivity and density, of several copper slag samples, from two different foundry plants.

## 1.1 General background: energy context

In the context of the increasing energy demand for the upcoming years considering the future population growth and development of economies, the WEO 2018 New Policies Scenario suggests a global energy demand rise by more than a quarter to 2040 [6]. These policies scenarios consist on the action of governments towards power generation handling and investments. Without improvements, a much stronger push up for electric mobility, electric heating and electricity access could lead to a 90% rise in power demand until 2040 [6]. Hence, the transition to global adoption of renewable energies is one of the important strategies for global leaders.

There are three key pillars for the improvement of the present and future renewable energy systems: affordability, reliability and sustainability. This concepts are closely interlinked, and each one needs to be approached differently depending on the weak points of renewable power technology to assess. For instance, cost-effective solutions for a reliable energy supply from solar power technologies, regardless of periods of low solar radiation.

Solar power technologies are one of the prospects for sustainable energy supply, due to

their low-emission and unlimited source characteristics. However, the mismatch between high thermal energy loads during the day, particularly on summer season, in contrast with the energy demand during early mornings, nights and specially on winter season, consists of a key-point for technological improvements. The two mainstream solar power technologies that currently adds capacity to the global energy grid, are photovoltaic (PV) and CSP technologies, both of which addresses the energy load and demand mismatch with energy storage systems, in addition, with efficiency improvements to leverage the solar resource. Commercial CSP plants are not as integrated into the market as it is for PV technology, though CSP has many prospects to be considered a valid substitute for fossil fuels, specially since it can concentrate solar radiation for high temperature TES (over 800°C), allowing higher power generation. Its current cost-effective disadvantages, unfolds around the initial inversion and limited upper temperature of operation, due to general storage materials, like oils and molten salts, starts decomposing around 400°C and 600°C, respectively. Therefore, new generations of TES technologies are studying the feasibility of packed-bed tanks, using air as HTF and recycled materials or industrial by-products, as a filler materials; in order to allow high power generation, flexible energy supply regarding the solar resource, with a relevant costs reduction.

## 1.2 Motivation

Since the integration of renewable energies to the global energy grid is one of the current subjects on climate change actions; it is important to study, develop, and implement, new alternatives to improve the current and future renewable energy projects, by diminishing the need of use of fossil fuels and other practices with negative environmental impact. These alternatives need to be cost-effective and feasible solutions, to the different issues regarding renewable energies, for thermal and electrical power generation.

It is known that solar energy is one the vastest energy resources in the world, with non-emission and inexhaustible supply characteristics. Solar energy is received by the earth about 200,000 times the world's total daily electric generating capacity [7]. Since it has potential to supply the increasing energy demand for upcoming years, it is relevant to improve and promote its integration to the global energy grid, taking into account, technical and economical challenges. Part of the main technical obstacles for solar power technologies, consists of improving the efficiency of the solar panel cells for PV systems, and high thermal capacity of TES for CSP. Both of these issues are the focus points to allow a flexible energy supply, regardless the geographical, seasonal conditions and daily variability. On a economical matter, the challenges for PV technologies unfold around the solar cells manufacturing and maintenance costs, as for TES systems, the selection of materials and storage medium, it heavily affects the design of the system and final inversion costs.

CSP is not a newly studied method, its integration to the global energy grid is not as extensive as compared to PV plants, since they were developed commercially around a decade of difference, (being one of the reason why CSP has a smaller magnitude of total installed capacity) [8]. One of the issues for CSP thermal energy storage, consists of new alternatives of materials for the storage medium. Most of CSP plants functioning nowadays utilizes molten

salts as heat sensible material and HTF, due to salts availability and high physical-thermal properties when melted. However, new TES materials and its application are being studied, for an overall more cost-effective CSP technologies. Some of the suggested options consists on the use of solid by-products from metal extraction industries, used as filler material for packed-bed TES configuration, which can reduce the materials procurement costs and allow a higher power generation due to their thermal properties. It is with this perspective, that this work is motivated by the possibility of using copper slag as filler material for packed-bed TES, specially since it is an abundant by-product from the mining industry, with high potential thermal capacities.

## 1.3 Objectives and Scope

### 1.3.1 General Objective

The main objective of this undergraduate thesis is to determine a reliable data base for copper slag's thermo-physical basic properties, in order to be used as a sensible heat material for packed-bed TES systems.

### 1.3.2 Specific objectives

To achieve the main objective, the following tasks must be completed:

- Determine previous information and characterization of copper slag
- Establish thermo-physical properties and their values to which compare the results of copper slag, specifically specific heat capacity, thermal conductivity and density, of conventional storage materials
- Determine and carry out the corresponding experimental equipment and methodology to measure properties
- Analyze the results and assess its potential in contrast to other storage materials alternatives

### 1.3.3 Scope

The present report is focused on the characterization of copper slag, since the high performance of other by-products have been proven, and considering the importance of mining industry in Chile and the amounts of copper slag produced during pyrometallurgical refining process; cooper slag suggests a potential application in CSP plants. The properties to determine are cooper slag's heat capacity, thermal conductivity and density, in order to create a thermodynamic analysis of different samples and configurations during the charge and discharge of a packed-bed coupled to a CSP system.

# Chapter 2

# Background of thermal energy storage systems

Thermal energy storage (TES), consists basically in a device that stores heat in a storage medium which can be a solid, liquid, or a combination of both. TES is mostly used in buildings, where heat is stored during the day and used to provide heat or thermal energy for domestic hot water in the later hours. Other common use of TES technologies is in industrial processes to store excess of thermal energy. Nevertheless, TES most practical usage is for solar energy storage, allowing to increase the effective use of thermal energy during the process of generating super-heated steam, to power conventional steam turbines and generate electricity, improving the overall reliability of the system.

The following chapter introduces theoretical background concerning the different technologies and design criteria for thermal energy storage systems; like different media types, storage concept and materials used for storing thermal energy, particularly for CSP technologies applications.

## 2.1 Storage concepts of TES

The basic stages of a TES system are three: charge, storage, and discharge of heat. These stages can take place simultaneously or more than once on a full cycle. Depending on this, and how the storage system is connected to the solar field, different storage concepts can be defined. Particularly, in solar power plants, the storage concepts can be classified in active and passive storage; active storage as well can be classified in direct and indirect systems [9].

### 2.1.1 Active storage systems

Active storage system utilizes forced convection in order to transfer heat to the storage material, and can be implement as a direct or indirect system.

### Active direct storage system

In an active direct storage system, the solar field and the storage concept are connected on a same circuit, as can be seen in Figure 2.1, allowing direct heat transfer to the power block from the solar field. On this case, the HTF operates simultaneously as the storage medium. These type of storage schemes utilizes two tanks; a "hot tank" for the heat load from the solar field, to use it eventually in periods of low solar radiation, and a "cold tank", to store the HTF that leaves the power block, which later is heated again in the solar field, closing the full heat charge and discharge cycle.

The advantages of a two tank implementation is the separation itself of the hot and cold storage, enabling a raise of the solar field output temperature to 450 - 500°C, thereby increasing the Rankine cycle efficiency of the power block steam turbine to 40% range (conventional plants have lower efficiency) [10].

The disadvantages are; high cost of the material used as a HTF and storage fluid; high cost of investment and maintenance of both tanks; relatively small temperature difference between the hot and cold fluid in the storage system; and high risk of solidification of the storage fluid, resulting in a increase of losses in the solar field due elevated temperatures [9].


Figure 2.1: Scheme of an active direct storage concept system [11]

### Active indirect storage system

On an active indirect storage system, the solar field and the storage system are separated in two circuits, thereby the HTF is a different substance from the storage material, and additionally an extra heat exchanger is required between these two sub-systems (see Figure 2.2).

Within the indirect storage concept design, there are two configurations: two-tank and single tank energy storage. The two-tank scheme is shown in Figure 2.2, where the HTF circulating in the solar field consists usually of molten salts, with a different storage fluid circulating in the TES area (generally oils). As in the previous case, the two-tank scheme has the same purpose of storing separately the the hot storage material from the cold storage,

furthermore the advantages are similar to the case of the direct system, excepting for the fact that the storage material flows only between hot and cold tanks and not throughout the solar field, allowing better maintenance strategies. The disadvantages are the same, plus a cost for the extra heat exchanger [9].

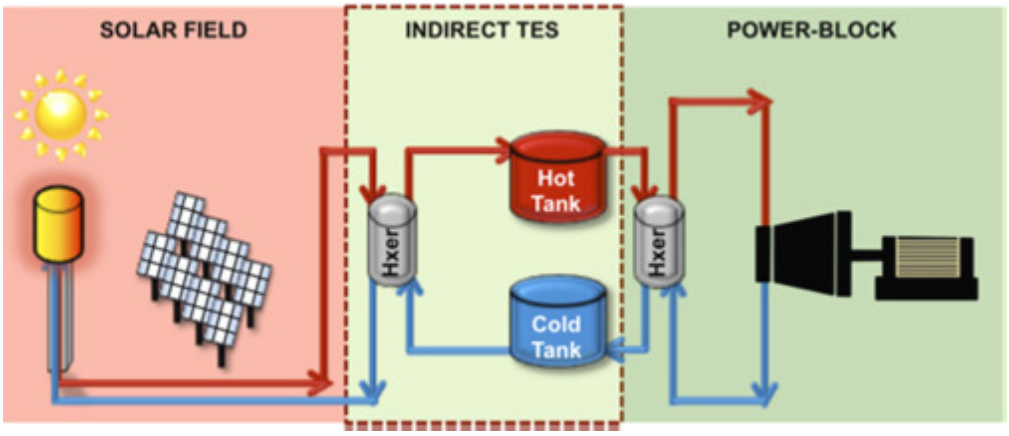


Figure 2.2: Scheme of an active indirect storage concept system [11]

The other indirect storage design concept, is to use a single tank with a solid filler material as the primary thermal storage medium, and a different HTF to allow the charge and discharge of heat. The single tank stores the hot and cold storage simultaneously, given the natural stratification of the HTF inside the tank due to convective phenomena, therefore, the hot storage sets on the upper part of the tank and the cold storage on the bottom. The transition layer between both zones is called thermocline.

The advantage of these systems, relies on the low cost of investment of a single tank, furthermore, the flexibility to chose a HTF allows to use air, which adds to the decrease in costs. Yet, the most significant cost reduction, is that the filler material is generally of a lower price (such as rocks and sand) resulting in a 35% reduction of costs than the two tank storage system [12].

On the other hand, the disadvantages are related to the difficulty of creating and keeping stable the thermocline; as well, the high outlet temperature drives to an increase of losses in the solar field; moreover, maintaining the thermal stratification requires controlled charging and discharging procedure, and appropriate methods and devices to avoid mixing; the overall design of the storage system is complex; and thermodynamically, it is an inefficient power plant according to [13].

### 2.1.2 Passive storage system

In passive storage systems, the storage materials are mainly made from concrete and castable materials; it does not participate "actively" from the charging and discharging of heat, that is to say, the medium itself does not circulate. What is more, a tubular heat exchanger is integrated into the material to transfer thermal energy from and into the HTF once it circulates through the storage medium (see Figure 2.4. These systems are also called regenerators [9].

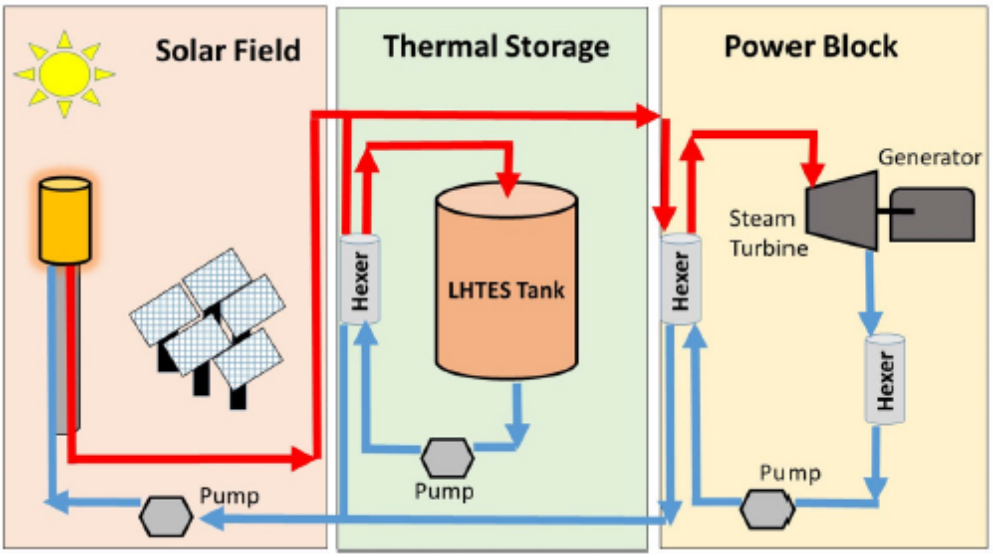


Figure 2.3: Scheme of an active indirect single tank storage concept system [14]

The main advantages of passive storage systems are low costs of thermal energy storage media; since the solid material is well compacted to the pipe heat exchanger inside it, heat transfer rates are high (into and out of the medium). The disadvantages are a long term instability; and increase of cost of heat exchanger and of engineering [9].

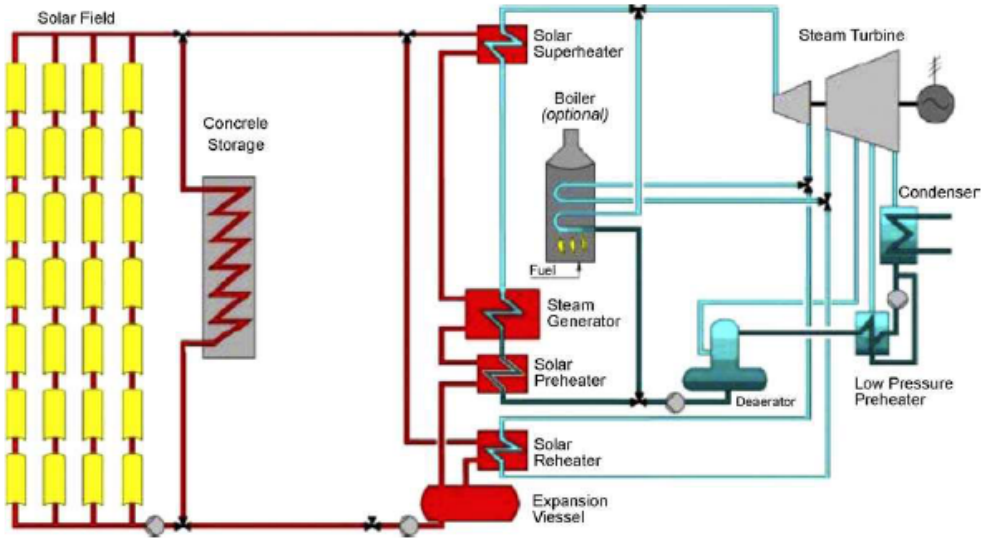


Figure 2.4: Scheme of a passive storage concept system [9]

## 2.2 Storage media and materials

TES systems can as well be classified on its storage media, that is to say, specifically how heat is stored in the material, weather it is on a physical or chemical approach. There are primarily three types of storage media: sensible heat storage, latent heat storage and chemical

heat storage. The materials chosen for each storage media require different thermal, physical, chemical and economic properties.

### 2.2.1 Sensible heat storage

Thermal energy can be stored in the change of temperature of a chosen medium, due to changes of its internal energy, without changing its phase. Moreover, the amount of heat stored in the material, is proportional to the temperature rise (or decrease) during the heat charging (discharging) process, hence the so-called heat sensible material.

The amount of thermal energy stored in a mass of material can be expressed as:

$$Q = \rho \dot{C_p} \dot{V} \dot{\Delta} T \tag{2.1}$$

Where $Q$ is the amount of heat stored in the material in $[J]$, $\rho$ is the density in $[kg/m^3]$, $Cp$ is the specific heat capacity in $[J/kgK]$, $V$ is the volume of the stored material in $[m^3]$, and $\Delta T$ is the temperature difference in $[K]$.

For the selection of a heat sensible material, the key parameter to analyze is thermal capacity, which is defined by the product of $\rho \times C_p$. According to H. Grirate et al. [15], thermal capacity dictates the thermocline storage system performances; high thermal capacity leads to high energy density, resulting in reduced storage vessel volume and cost. On another note, other relevant properties for the selection of a storage material are: thermal conductivity, thermal diffusivity, thermal stability, temperature range of operation, costs of implementation, amongst others; which contribute as well on the total storage thermal capacity, and its practical integration to another system (solar field or power block).

Sensible heat storage materials can be liquid or solid. The first one usually is simultaneously used as HTF (dual storage), while the latter requires a separated liquid medium as HTF. The most studied solid materials alternatives for TES are concrete and castable ceramics, mostly due to their low price and high thermal capacity. Table 2.1 shows the main solid materials studied and characterized for TES found in literature.

Table 2.1: Solid materials alternatives for heat sensible storage [16, 17].

| Storage medium | Temperature | | Average density $[kg/m^3]$ | Average heat conductivity $[W/mK]$ | Average heat capacity $[kJ/kgK]$ | Volume specific heat capacity $[kWh_t/m^3]$ | Media costs per kg $[US\$/kWh_t]$ |
|---|---|---|---|---|---|---|---|
| | Cold [°C] | Hot [°C] | | | | | |
| Sand-rock mineral oil | 200 | 300 | 1700 | 1.0 | 1.30 | 60 | 0.15 |
| Reinforced concrete | 200 | 400 | 2200 | 1.5 | 0.85 | 100 | 0.05 |
| NaCl (solid) | 200 | 500 | 2160 | 7.0 | 0.85 | 150 | 0.15 |
| Cast iron | 200 | 400 | 7200 | 37.0 | 0.56 | 160 | 1.00 |
| Cast steel | 200 | 700 | 7800 | 40.0 | 0.60 | 450 | 5.00 |
| Silica fire bricks | 200 | 700 | 1820 | 1.5 | 1.00 | 150 | 1.00 |
| Magnesia fire bricks | 200 | 1200 | 3000 | 5.0 | 1.15 | 600 | 2.00 |

Apart from castable ceramics, concrete is one of the solid materials alternatives with better thermal properties for TES, since it has a low cost, facility of handling, and structural

stability. Regardless of its relatively low thermal conductivity, concrete has relatively high thermal capacity. Studies by the DLR in Stuttgart have shown that a new high temperature concrete, resulted on better thermal properties than regular concrete. The comparison between high temperature concrete and castable ceramics properties are shown in Table 2.2 [18].

Table 2.2: Material properties of storage materials developed at DLR (Stuttgart, Germany)[18]

| Material | Castable ceramic | High temperature concrete |
|---|---|---|
| Density [kg/m3] | 3500 | 2750 |
| Specific heat at 350°C [J/kgK] | 866 | 916 |
| Thermal conductivity at 350°C [W/mK] | 1.35 | 1.0 |
| Coefficient of thermal expansion at 350°c [10-6/k] | 11.8 | 9.3 |

Amongst the different liquid alternatives to transfer heat that have been studied, such as water, air, oil, and sodium; molten salts offered the highest thermal properties results. The so-called solar salt, is a binary salt consisting of 60% $NaNO_3$ and 40% $KNO_3$. The specific composition and concentration of these salts can vary depending on the commercial supplier and application. For example, HitecXL is a commercial ternary salt consisting of 48%$Ca(NO_3)_2$, 7%$NaNO_3$ and 45%$KNO_3$, which have been used before in non-solar applications [19]. Nowadays solar salts used in solar power systems are not flammable and non-toxic; their fusion point is around 221°C, and can be kept in liquid state at 288°C in a insulated cold storage [9]. Solar salts upper temperature limit before decomposing, is about 100°C higher than oils (see Table 2.3), allowing a wider range of temperature for higher temperature storage performance.

Molten salts are used simultaneously as HTF and storage material, and most of nowadays CSP installed plants utilize molten salts as its principal TES resource. Despite their high thermal properties, like specific heat capacity and relatively higher density than oils, as shown in Table 2.3, their high freezing point becomes a disadvantage in terms of heat losses and risk of obstruction due to solidification in the circuit, resulting in expensive piping materials. Solar salts lower thermal conductivity also involves a higher investment on more complex heat exchangers. As such, the desired characteristics of molten salts consists of high density, low vapour pressure, moderate specific heat, low chemical reactivity, and low cost; of which only a limited number of molten salts accomplish these requirements [13, 20].

Table 2.3: Liquid materials alternatives for sensible heat storage [16, 17]

| Storage | Temperature | | Average density | Average heat conductivity | Average heat capacity | Volume specific heat capacity | Media costs per $kg$ | Media costs per $kWh_t$ |
|---|---|---|---|---|---|---|---|---|
| | Cold $[^oC]$ | Hot $[^oC]$ | $[kg/m^3]$ | $[W/mK]$ | $[kJ/kgK]$ | $[kWh_t/m^3]$ | $[US\$/kWh_t]$ | $[US\$/kWh_t]$ |
| HITEC salts | 120 | 133 | - | - | - | - | - | - |
| Mineral oil | 200 | 300 | 770 | 0.12 | 2.6 | 55 | 0.30 | 4.2 |
| Synthetic oil | 250 | 350 | 900 | 0.11 | 2.3 | 57 | 3.00 | 43.0 |
| Silicone oil | 300 | 400 | 900 | 0.10 | 2.1 | 52 | 5.00 | 80.0 |
| Nitrite salts | 250 | 450 | 1825 | 0.57 | 1.5 | 152 | 1.00 | 12.0 |
| Nitrate salts | 265 | 565 | 1870 | 0.52 | 1.6 | 250 | 0.50 | 3.7 |
| Carbonate salts | 450 | 850 | 2100 | 2.0 | 1.8 | 430 | 2.40 | 11.0 |
| Liquid sodium | 270 | 530 | 850 | 71.0 | 1.3 | 80 | 2.00 | 21.0 |

### 2.2.2 Latent heat storage

Latent heat storage is based on storing thermal energy in the phase change of a material with solid-liquid transition. High amounts of energy can be stored in a short temperature difference (almost isothermally), allowing charging and discharging of heat with lesser heat losses than sensible heat storage (see Figure 2.5), thereby, is more efficient in an energy point of view. The materials used in this type of storage are called phase change materials (PCM), moreover, the preferable phase change for storage is the transition solid to liquid of the medium.

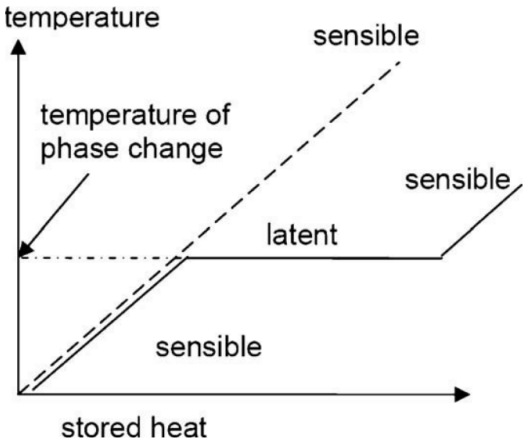


Figure 2.5: Phase change profile of PCM [21]

While PCM have a higher energy density; therefore, allows large amounts of energy to be stored in relatively small volumes; the design criteria for heat transfer and storage is more difficult since there is a limited storage medium selection (see Table 2.4), with possible degrading performance after a large number of freeze-melt cycles. In addition, PCM have low thermal conductivity leading to slow charging an discharging rates [22, 23]. Nevertheless, the potential improvement of energy efficiency of PCM storage is very much possible, by adding composite latent heat storage materials (CLHSM), with greater thermal conductivity, or by improving heat transfer by convection.

Table 2.4: Commercial PCM from EPS (United Kingdom) and Rubitherm (Germany) [24]. *n.a.: not available.

| Name | Type | Manufacturer | Phase change temperature $[^oC]$ | Density $[kg/m^3]$ | Latent heat $[kJ/kg]$ | Specific heat $[kJ/kgK]$ | Thermal conductivity $[W/mK]$ |
|---|---|---|---|---|---|---|---|
| RT110 | Paraffin | Rubitherm | 112 | 213 | n.a. | n.a. | n.a. |
| E117 | Inorganic | EPS | 117 | 1450 | 169 | 2.61 | 0.70 |
| A164 | Organic | EPS | 164 | 1500 | 306 | n.a. | n.a. |

### 2.2.3 Chemical heat storage

This type storage consists of using the heat of chemical reactions of a medium, allowing a higher energy efficiency of the charging and discharging processes. In order for this to

happen, the chemical reaction involved must be completely reversible.

The advantages of this storing option are high storage energy densities, indefinitely long storage duration at near ambient temperature, and heat-pumping capability. However, chemical heat storage is still on its early stages of development.

Table 2.5 shows the some of the chemical reactions that have been investigated. Nevertheless, the most important reactions that have been considered are: reactions metal oxide/metal ($SnO_x/Sn$) and ammonia [9].

Table 2.5: Chemical storage materials [9]. *n.a.: not available.

| Compound | Material energy density | Reaction temperature [$^oC$] |
|---|---|---|
| Ammonia | 67 [$kJ/mol$] | 400-500 |
| Methane/water | n.a. | 500-1000 |
| Hydroxides, e.g. | 3 [$GJ/m^3$] | 500 |
| Calcium carbonate | 4.4 [$GJ/m^3$] | 800-900 |
| Iron carbonate | 2.6 [$GJ/m^3$] | 180 |
| Metal hydrides | 4 [$GJ/m^3$] | 200-300 |
| Metal oxides (Zn and Fe) | n.a. | 2000-2500 |
| Aluminium or alumina | n.a. | 2100-2300 |
| Methanolation-demethanolation | n.a. | 200-250 |
| Magnesium oxide | 3.3 [$GJ/m^3$] | 250-400 |

### 2.2.4 Properties requirements of storage materials

There are basic properties and characteristics a storage material for TES must accomplish. The following properties are the ones to considerate in order to select a potential alternative, specifically for sensible heat storage, since this is the type of storage material that the present work is focusing on.

#### Thermo-physical properties

- Range of operating temperature fitted to exclude the phase change of the material: For CSP technologies, the maximum operating temperature can vary from 250 to 750°C or higher, depending on the receiver concept (parabolic trough, parabolic dish, solar tower) and among other technical considerations [25]. The storage material, weather is solid or liquid, needs to maintain its phase regardless of the temperature throughout the day. To put it in context, molten salts have a relatively high freezing point (between 120 and 220°C depending on the mixture), if the medium reaches a lower temperature, the system risks technical problems due to solidification in pipes and heat exchangers. It may also lead to important heat losses, specially at night in deserted regions or high altitude areas, where CSP technology allocation is more appropriate. Similarly, is important to establish the upper temperature limit of operation, since it defines the power output of the CSP system. Therefore, it is preferably that the chosen material can operate to the highest temperature possible, without decomposing itself and jeopardizing its thermal performance.

- High specific heat capacity ($Cp$): One of the most important requirements for a sensible heat material, it is their ability to store high amounts of energy within a small quantity of mass, and through a small temperature difference.
- High thermal conductivity: An efficient and proper transport of thermal energy is desirable, when considering that heat must be charge to- and discharge from- the storage material, despite that in a heat loss perspective, a small thermal conductivity is the preferable option.
- Thermal stability: This property consists of the resistance to degradation of the material to an increase of temperature, in other words, little to none mass gain or losses. It is preferable that the chosen material behaves thermally stable during consecutive heating and cooling cycles, and on a long term basis.
- High density: Since thermal energy needs to be stored preferably in high quantities on small volumes, a high density is desirable for better thermal capacity, like described in equation Equation 2.1.

**Chemical properties**

- Long-term chemical stability: The chosen materials needs to preserve its chemical composition under heat charge and discharge, and repetitive thermal cycles, in order to not exposed the system to unexpected chemical reactions or undesirable chemical products (like corrosive compounds).
- Compatibility with container: Solid and liquid storage materials, require to be chemically compatible with the container and constructive materials in general, to avoid corrosion after several thermal cycles.
- No toxic, no flammable, no pollutant: For environmental y safety reasons.

**Economic properties**

- Low cost: Requires to be cost-effective, in order to be competitive to other commercial alternatives of storage materials.
- Abundant and available.

# Chapter 3

# Literature review

The following chapter presents a review about the studies carried out on copper slag characterization, and other by-products from the steel making industry, focusing on their potential as sensible heat materials for TES.

The purpose of this literature review is to gather information about copper slag characterization, and other sensible heat materials alternatives, in such a way as to compare and validate the results obtained in this work. Furthermore, this review focuses as well, on establishing suitable experimental methodology for copper slag characterization, based on the proven approach by different authors.

## 3.1 Copper slag TES related studies

In order to characterize the thermo-physical properties of copper slag, and assess its potential as sensible heat material, it is important to establish prior information on this material, specially around TES context.

### 3.1.1 First registered approach

The first proposal of a design of a CSP project plant, using copper slag as sensible heat material, was presented in 1980 at the Third Miami international conference on alternative energy sources. The proposal of Paul A. Curto and George Stern [26], former employees of Gibbs & Hill, Inc. (a non active company nowadays), considered the utilization of copper slag, due to its prospective high thermal properties, since is a by-product with high percentage of ferrous compounds. Furthermore, for at that time, copper slag had no cost value and no subsequent utilization, it was a disposal material with high availability.

Copper slag's application was considered as a filler material in a packed-bed configuration TES, to be potentially used in gas power cycles and industrial processes; since it could

be used in a relatively high operation temperature range, from 650°C up to 1200°C, and remaining chemically, thermally and mechanically stable. Some of the conclusions of the characterization study by Curto and Stern, stated that copper slag is a material with a relatively high thermal capacity. It presented a specific gravity of 4.3 to 4.4, and a specific heat capacity range from 0.670 to 1.004 $[J/gK]$, over the range of 20 to 1000°C.

The packed-bed tank design that was assessed in the study; with 30 meters of diameter and 30 meters of length, packed with 2 to 6 centimeters of copper slags; showed an impressive performance (as it was predicted). Air was used as the working fluid, with a thermocline of only a few meters thick, exhibiting a temperature delta over 500°C. The storage capacity was sufficient to provide 6000 standard cubic meters of air flow at 540°C, for up to three days at continuous discharge.

Despite as much as copper slag had potential for cost-effective high TES, due to lack of funding for solar technology development at the time, the project did not reach to its test model phase. What is more, the design work and engineering drawings of the project, were destroyed on 9/11, when the twin towers collapsed in Manhattan, where Gibbs  Hills, Inc. was situated. Since then (around a breach of 30 years later), copper slag characterization as sensible heat storage material has been studied by only a few authors.

### 3.1.2 Copper slag characterization

The studies concerning copper slag's characterization presented in this work, address two main issues; the first one being the comparison of thermal properties of different recycled materials (where samples of copper slag are included), and the second one consists of copper slag implementation as an aggregate to different composite configurations; both of which depict a general view on copper slag's properties.

For instance, in the case study of M. Navarro et al. [5], for the selection and characterization of recycled materials for TES, different by-products from the mineral and metal industry were studied, among these, two samples of copper slag were characterized, as well as mortar formulations using three types of cements and copper slags aggregates, in a proportion of 75 to 80% of the mixture. These materials were assessed in their basic thermo-physical properties (see Table 3.1), where $k$ represents thermal conductivity, $Cp$ specific heat capacity and $\rho$ the density of the material. Only the results of the study related to copper slag, and its use as an aggregate, are shown in the following table.

Copper slag samples considered in this analysis are named Slag P and Slag B. Since their compression and molding were not possible, their preparation method consisted of powders. In addition, they were included as aggregates in mortar formulations, using as binders Portland, aluminous and phosphate cements. Results from the experimental analysis for each property and material are resumed in Table 3.1. Specific heat capacity ($Cp$) results from DSC analysis are listed at different working temperatures (100 - 300 - 500 °C). Thermal conductivity ($k$) was measured at 20°C. From these results, it was observed that samples which preparation method consisted of powder, presented lower values compared to the mortar formulations. This is due to the porosity of the powder samples, where air plays a significant

Table 3.1: Properties of different studied thermal energy storage materials [5].

| Sample | Preparation method | $k$ $[W/mK]$ | Cp $[J/gK]$ | | | $\rho$ $[kg/m^3]$ | Cost $[euro/kg]$ |
|---|---|---|---|---|---|---|---|
| | | | 100°C | 300°C | 500°C | | |
| Slag_P | Powder | 0.8 | 0.571 | 0.683 | 1.188 | 3600 | 0.15 |
| Slag_B | Powder | 1.1 | 0.648 | 0.633 | 0.999 | 3700 | 0.15 |
| CBPC_B | Mortar formulation | 1.6 | 0.703 | 0.861 | 1.015 | 2828 | 0.15 |
| CBPC_P | Mortar formulation | 1.5 | 0.655 | 0.780 | 1.230 | 2804 | 0.15 |
| AB | Mortar formulation | 1.4 | 0.640 | 0.730 | 0.923 | 3030 | 0.15 |
| AP | Mortar formulation | 1.4 | 0.630 | 0.752 | 0.985 | 2947 | 0.15 |
| PP | Mortar formulation | 1.4 | 0.623 | 0.619 | 0.971 | 2785 | 0.12 |
| PB | Mortar formulation | 1.8 | 0.681 | 0.582 | 0.829 | 2859 | 0.12 |

role on decreasing thermal conductivity. Nevertheless, these results are relatively higher than conventional sensible heat materials, which are listed in Table 2.1 and Table 2.3 in the previous chapter. On the other hand, $Cp$ results were relatively lower, however considering that densities were higher and costs per unit of mass were lower, therefore they were concluded to be feasible alternatives for sensible heat storage materials.

Another characterization approach of copper slag consists of a chemical composition characterization, which has been presented in epoxy composites studies, where copper slag is used as filler material to improve mechanical properties of composites, like thermal conductivity and wear resistance. In Aamir Shams's project report [27], Table 3.2 is formulated as a resume of the typical chemical composition of copper slag, based on the case study of Biswas et al. [28] and Gorai et al. [29].

Table 3.2: Typical chemical composition of copper slag [27].

| | | | |
|---|---|---|---|
| Fe | 30-40 | Tin | 0.08 |
| SiO2 | 35-40 | Antimony | 0.07 |
| Al2O3 | <10 | Chromium | 0.02 |
| Zn | <1 | Cobalt | 0.02 |
| CaO | <10 | Nickel | 0.02 |
| Cu | <2.1 | Cadmium | 0.04 |
| MgO | >1.5 | Arsenic | Not Detected |
| TiO2 | <2 | Beryllium | Not Detected |
| Free Silica | <1 | Trace elements | <0.5 |
| Lead | 0.1 | Moisture | <1 |

Copper is pyrometallurgically extracted from ore loads, which composition is primarily from sulphides and oxides of iron and copper. During matte smelting, sulfidisation of copper and iron results in the formation of $Cu_2S$ and $FeS$. The latter keeps reacting and oxidizing, to the point that when silica ($SiO_2$) is added to the smelting process, it forms what is known as slag, which is primarily a composition of $FeO$ and $SiO_2$. Silica is added in the melted matte (at over 1300°C) to isolate the copper sulfides from the rest of the compounds. Then, a certain amount of lime and alumina are added to stabilize the slag structure, and later discharged from the furnace to cool naturally [30]. Other compounds in smaller concentration are presented as well in Table 3.2, like calcium oxide and small percentage of residual copper (less than 2%). The values presented in this table is a general composition of copper slag, the specific proportions of these compounds depend mainly on the composition of the mine site.

Table 3.3 shows some of copper slag's physical and mechanical properties presented by Gorai et al. [29]. The specific gravity range varies with iron content, and its bulk density is higher than that of conventional aggregates.

Table 3.3: Copper slag properties as presented by Sham's study [27].

| Appearance | Specific gravity | Absorption, % | Bulk density $[kg/m^3]$ | Conductivity $[\mu s/cm]$ |
|---|---|---|---|---|
| Black, glassy, more vesicular when granulated | 2.80 - 3.80 | 0.13 | 8.99 - 10.11 | 500 |

Copper slag in these studies is considered as an aggregate, depending on the property to analyze or improve of the composite, only some properties of copper slag were evaluated, hence the lack of results considering thermal properties. Nonetheless, results from Table 3.2 and Table 3.3 gives a chemical perspective of copper slag, required to have in consideration in the result analysis of this work. On the other hand, the results obtained by Navarro et al. [5] are the basic properties and indicators to consider for the selection of a sensible heat storage material, that is to say: specific heat capacity, density, thermal conductivity, and costs associated to the material. However, the values of these properties can vary depending on the provenience of the ore load from which the slag was obtained, as well as between each sample, since is a heterogeneous by-product. Taking this into account, the results obtained by Navarro et al. [5] are sufficient to compare copper slag to other recycled materials, and offer a first approach on the characterization of copper slag.

## 3.2 Industrial by-products characterization for TES

The study of new sensible heat materials for TES has been focused on the characterization of by-products from the metal and mining industry, since they represent a low cost and largely available option. Different authors have studied slags from the iron and steel industry, to use them as filler material in a packed-bed TES configuration, mainly because these by-products have already been through high temperature processes (up to melting points of 1000°C), therefore, they are likely thermally stable, which results in an attractive alternative for high temperature TES for CSP.

The properties that need to be assesses for the characterization of storage materials consist of: specific heat capacity, thermal conductivity, thermal diffusivity and density. Chemical stability and thermal stability, and other properties like corrosion and wear resistance, are also relevant, however they need to be taken into account in a long term performance perspective of the TES, after several heat charge and discharge cycles.

The corresponding methodology and results from the articles related to the characterization of different storage materials alternatives, are addressed hereunder by the thermophysical properties.

### 3.2.1 Density

In materials like slags, porosity is a variable that needs to be taken into account, specially distribution and size of the pores, which can change from a sample to another. Bulk density, or apparent density in this case, considers pores volume inside the material, while skeletal density subtracts them from the final volume, resulting in a higher value than bulk density. Skeletal density is considered as the real density of the sample.

In the thermo-physical characterization of electric arc furnace (EAF) slags made by Ortega, Calvet, et al. [3], apparent and skeletal density of two sample of these slags (Slag 1 and Slag 2) were measured, before and after they were thermally treated at 1000°C for 24 hours in air as atmosphere, for furthermore, analyze oxidation effects in their structure. Table 3.4 shows the results of this property, showing a decrease of density after oxidizing. Additionally, skeletal density proved to be higher than apparent density.

Table 3.4: Apparent and skeletal density of EAF slags before and after oxidation [3]

| Density $[kg/m^3]$ | Slag 1 | | Slag 2 | |
|---|---|---|---|---|
| | Raw | After oxidation | Raw | After oxidation |
| Apparent | 3650 | 3430 | 4110 | 3770 |
| Skeletal | 3880 | 3860 | 4260 | 4030 |

In the case study of Agalit et al. [31], samples of induction furnace slag (IFS) were characterized thermally and chemically. Bulk density was measured using the pycnometer method. The average result is presented in Figure 3.1 as well as other bulk density values presented in literature.

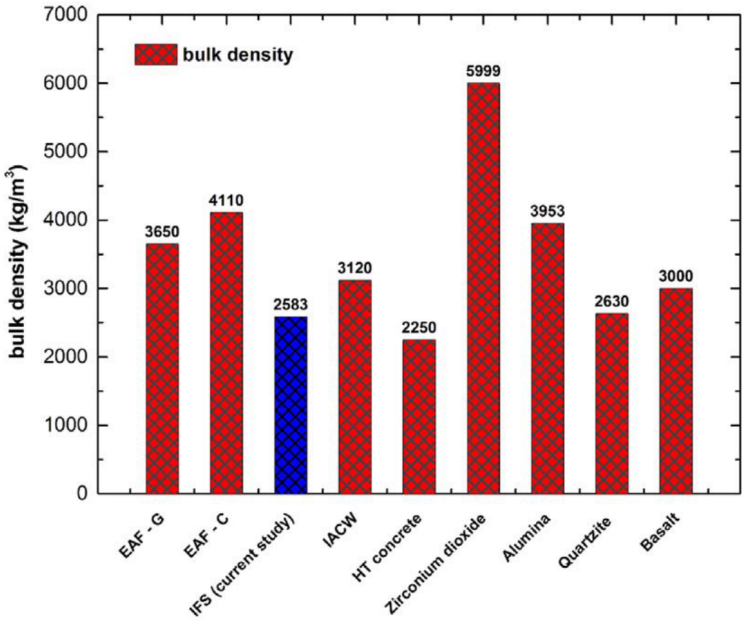


Figure 3.1: Bulk density values of the as-received IFS and high temperature storage materials [31].

Another characterization of EAF slag was conducted by Gil et al. [32], where the average (apparent and skeletal) density results are shown in Table 3.5. Skeletal density was measured

by the pycnometer method, and apparent density was measured through an Archimedes method. The difference between these densities indicates a strong porous nature, which might be related to crystallization process of this material. Additionally, samples in this study were measured before and after re-melting and cooling them, however no significant difference was concluded.

Table 3.5: Density of EAF slags studied by Gil et al. [32]

| Density $[kg/m^3]$ | As received | Remelted |
|---|---|---|
| Apparent | 3170 | 2860 |
| Skeletal | 3510 | 3600 |

### 3.2.2 Thermal and chemical stability

Thermal stability depicts the resistance of the material to degradation within a temperature range. This type of property is commonly studied through thermal gravimetric analysis (TGA), which consists of measuring the sample's mass throughout a heating or cooling process over a defined temperature range. Generally a triple run cycle is conducted to determine if the material stabilizes. Weather the sample's mass varies considerably during these cycles, it can be determined if any relevant reactions are occurring. For instance, in the case study of Ortega, Faik, et al. [4], the samples of EAF slags were tested through a heating and cooling cycle and a second heating afterwards (see Figure 3.2. The TGA results showed an increase in mass of 3% for EAF slag 1 and 5% for EAF slag 2. However, no relevant mass change is observed in the subsequent cooling and heating part of the cycle.

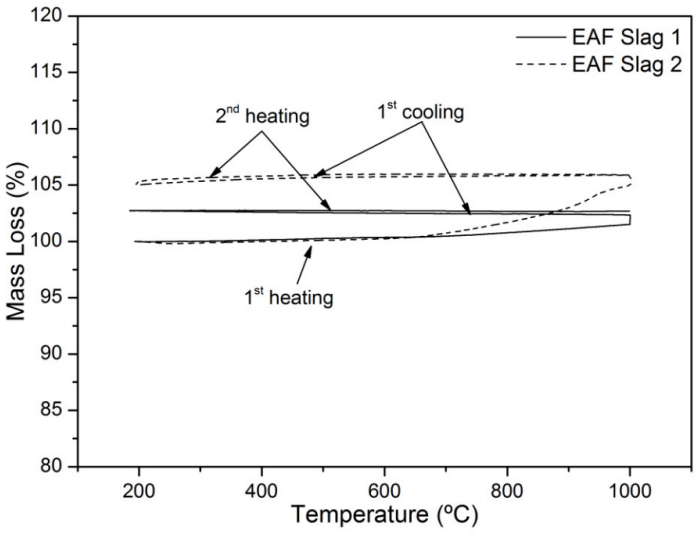


Figure 3.2: Thermogravimetrical analysis of slags by Ortega, Calvet, et al. [4]

According to Ortega's analysis, the mass increase during the first heating curve corresponds to the oxidation of some metallic (iron) parts and some metal oxides, with low oxidation rates, that are presented in the slag. The reason why during the second heating curve there was no important mass variation, it is due to these elements were totally oxidized,

stabilizing the samples. As a consequence, it was concluded that the material after the first heating run is thermally stable, at least, up to 1000°C [4].

On another article by Ortega, Calvet, et al. [3], two other samples of EAF slag were analyzed, with the variation that they were measured during 3 heating-cooling cycles. The curve results presented in Figure 3.3 and Figure 3.4 showed that, similar to the previous cases, the samples increased their mass during the first heating run, around 3.5% for slag 1 and 5.6% for slag 2. This mass gain is due to oxidation of the metal oxides elements in the slag, reaching a higher oxidation rate with temperature. However, no further mass changes were observed during the second and third heating run, therefore, it was concluded that the samples reached thermal stability up to at least 1100°C after the first heating and cooling cycle [3].

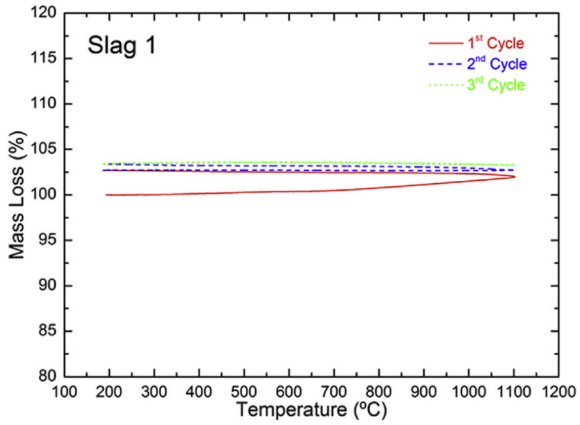


Figure 3.3: Thermal gravimetric analysis of slag 1 [3]

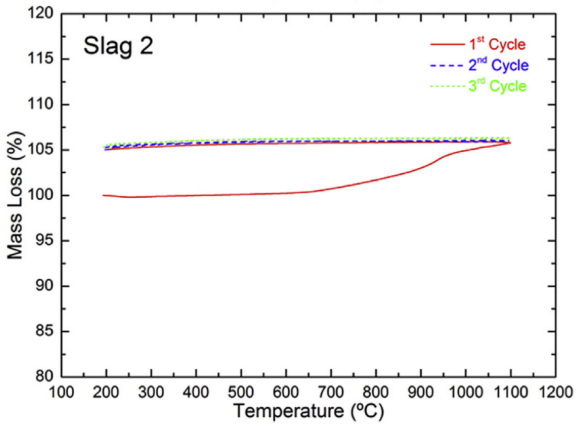


Figure 3.4: Thermal gravimetric analysis of slag 2 [3]

The same conclusion was obtained by Wang et al. [33] when analyzing two samples of EAF slags. S slag and C slag (named after their provenance from Spain and China, respectively), were analyzed during 3 heating-cooling cycles, from 100°C to 1000°C. Figure 3.5 and Figure 3.6 show the TGA results. During the first thermal cycle, the mass of C slag decreased slightly about 1.31% of the sample's weight, with increase of temperature. This could be caused by water evaporation or reduction of some components. During the following heating and cooling cycles, TGA results showed insignificant mass increase, around 1.54% for C slag, and 2.02% for S slag. After the third cycle of both samples, they were concluded to become thermally stable up to 1000°C [33]. Equivalent to both articles by Ortega, Faik, et al. [4] and Ortega, Calvet, et al. [3], the increasing mass is related to oxidation of the iron components of the samples, which allowed them to become more stable.

Since these slags are by-products of an already high temperature process, they've been thermally stabilized beforehand. The mass increase occurs particularly due to oxidation of the outer surface, hence the small mass variation in the previous results. This analysis was also considered in the case study of Navarro et al.[5]. The copper slag samples, and the mortars made from them, were tested showing thermal stability after 200°C up to 800°C. As can be observed in Figure 3.7, the copper slag sample (slag B) showed a small increase in mass in contrast with the mortar samples, whose mass decreased around 8 to 10%, mainly caused by water evaporation of the mortars.

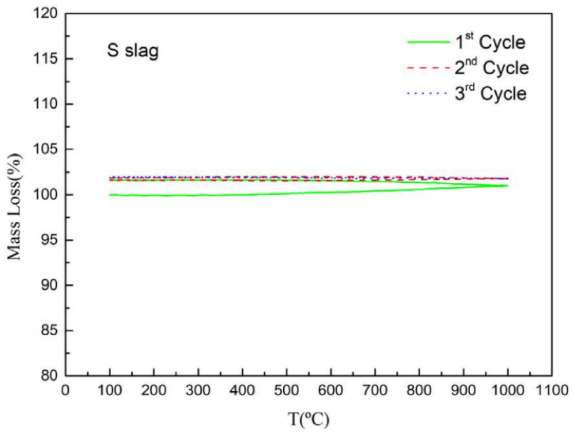


Figure 3.5: Thermal gravimetric analysis of slag S [33]

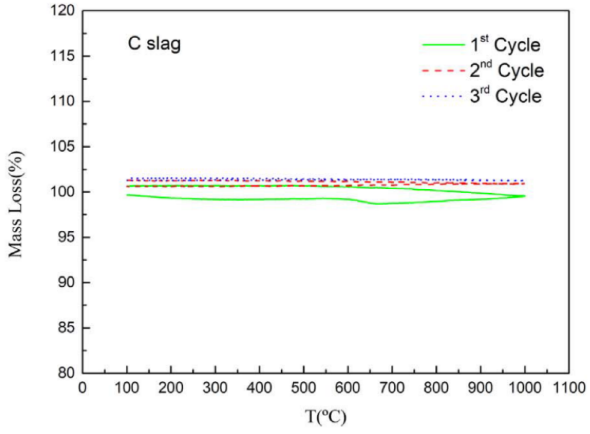


Figure 3.6: Thermal gravimetric analysis of slag C [33]

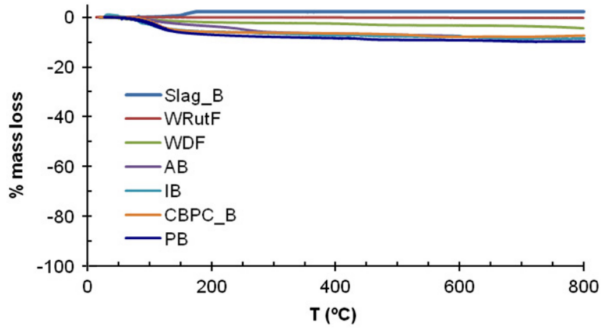


Figure 3.7: TGA analysis results for copper slag and mortars [5]

To properly determine if a material is chemically stable, it needs to be cooked at high temperature for several hours, in order to analyze its chemical composition before and after being cooked, this way it can be determined if the material on the matter is having any decomposition or change in its initial proportion of components. Ortega, Calvet, et al. [4] analyzed EAF slags chemically before and after being thermally treated, by putting pebbles of slag in a chamber furnace at 1000°C for 500 hours. The samples were analyzed on their structure, by X-ray powder diffraction (XRD), superficial analysis with Scanning Electron Microscopy (SEM) and Energy-dispersive X-ray (EDX) spectroscopy. It was concluded that the materials after 500 hours didn't show any corrosion (considering air as HTF), since the XRD patterns of the slags did not show important structure variations. Furthermore, the values of the auto-refined lattice parameters of detected phases, before and after the compatibility tests, were the same. The slags were concluded to be chemically stable [4].

### 3.2.3 Specific heat capacity

Specific heat capacity ($Cp$) is generally measured and determine through differential scanning calorimetry (DSC) analysis, throughout a temperature range. In the slag characterization of Ortega, Calvet, et al. [4], after being thermally treated and stabilized, $Cp$ was analyzed through DSC analysis. The results obtained for EAF slag 1 and slag 2 (at 350°C),

were 865 $J/kgK$ and 837 $J/kgK$, respectively. In this case, they focused on obtaining a single value for $Cp$, for practical reasons, in order to use it in an analytical model of TES presented in the same paper. Nevertheless, in Ortega's later study, a $Cp$ curve was obtained through DSC analysis, in a temperature range from room temperature (RT) to 500°C. Additionally, a LFA (laser flash apparatus) procedure was conducted to complement results in a higher temperature range, from 500°C to 1000°C. The results showed a $Cp$ increase, as can be seen in Figure 3.8. For both slag samples, $Cp$ values are very similar up to 250°C, then the curve for slag 1 reached slightly higher values, to later present a constant behaviour at a higher temperature range, generally related to thermal saturation. On the other hand, slag 2 shows a decrease on $Cp$ values around 700°C. This behaviour can be related to phase transition in the sample. Both of the slag samples reached a saturated point, with a $Cp$ of 950 $[J/kgK]$ and 890 $[J/kgK]$, for slag 1 and slag 2, respectively.

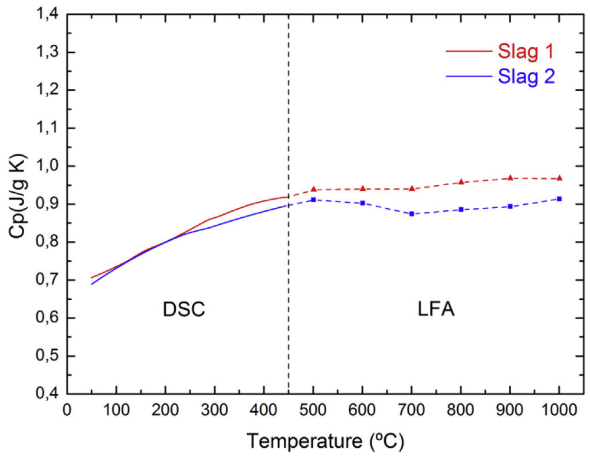


Figure 3.8: Experimental specific heat capacity of the EAF slags, through DSC and LFA analysis [3]

In the study of Wang et al. [33], the $Cp$ curve obtained by DSC analysis is shown in Figure 3.9, within a temperature range from RT to 500°C. There is an increase of $Cp$ with temperature. The $Cp$ curve for C slag increased from 0.717 $[J/gK]$ to 0.975 $[J/gK]$, and for S slag it increased from 0.713 $[J/gK]$ to 0.858 $[J/gK]$; both of which ranges are similar to the results presented by Ortega, Faik, et al. [3] in Figure 3.8.

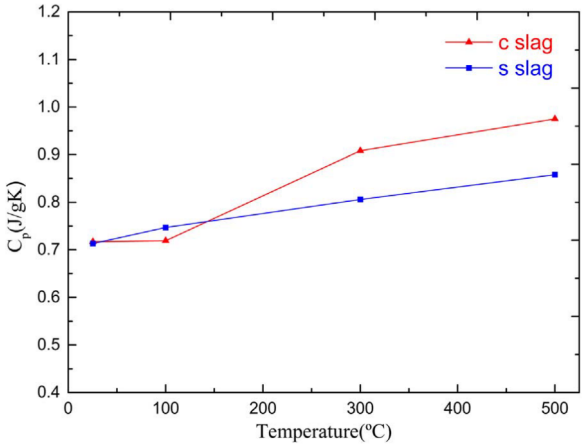


Figure 3.9: Specific heat capacity results from RT to 500°C, of EAF slags [33].

The increasing of $Cp$ with temperature was also observed in the characterization study of IFS by Agalit et al. [31]. Similar to the other studies, the resulting curves showed a changed of the rate at which $Cp$ was increasing, until reaching a constant behaviour. This behaviour can be explained by: as $Cp$ is an intrinsic property of vibration amplitudes of the different chemical bonds present in a certain material; thus these amplitudes increase as function of temperature to reach a saturation point [31].

### 3.2.4 Thermal conductivity and thermal diffusivity

To measure thermal conductivity ($k$) and thermal diffusivity ($\alpha$), different technical approaches can be utilized. For example, thermal conductivity of EAF slags, from Ortega, Faik, et al. [4], were calculated by using the following equation:

$$k = \alpha \times \rho \times Cp \tag{3.1}$$

Thermal diffusivity results were obtained from LFA measurements. The resulting thermal conductivity was 1.47 $[W/mK]$ and 1.51 $[W/mk]$, for EAF slag 1 and EAF slag 2, respectively (at a temperature of 350°C). However, thermal conductivity is not a constant property independent of temperature, which was observed in the later investigation of Ortega, Faik, et al. [3]. Thermal diffusivity was measured through a temperature range from 100 - 1000°C, with a step of 100°C. The curves for thermal diffusivity (continuous lines) and thermal conductivity (discontinuous lines) are shown in Figure 3.10 [3].

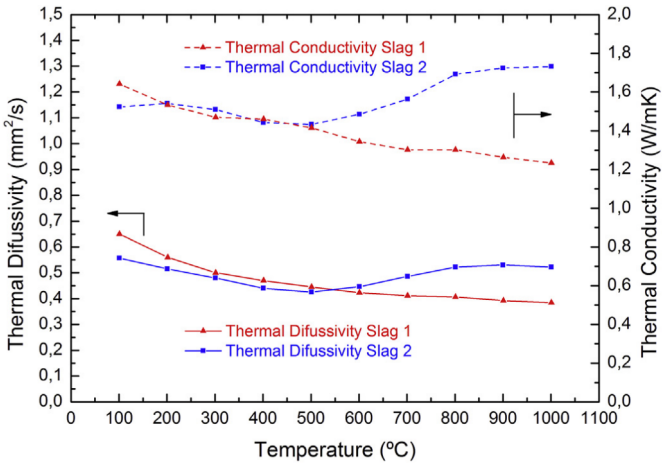


Figure 3.10: Thermal conductivity and thermal diffusivity curves of EAF slags [3]

In Figure 3.10, both slags behaved similarly at temperatures lower than 500°C, after this point the curves started to separate: the thermal conductivity curve for slag 1 decreased, and for slag 2 increased. This is a result from different crystal structure presented by both slags in Ortegas's characterization. Crystalline slags show a decrease of thermal diffusivity with temperature, whereas for glassy slags, shows a nearly constant value of thermal diffusivity [34]. Which is coherent to the results from Figure 3.10, since Slag 1 has a lower crystallinity than slag 2, as it was analysed in Ortega's results for XRD [3].

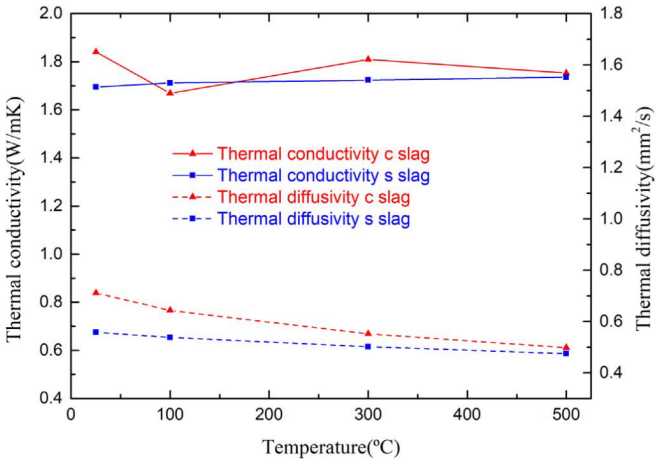


Figure 3.11: Thermal conductivity and thermal diffusivity curves [33]

In the characterization study of Wang et al. [33], thermal conductivity was obtained as well through LFA, by measuring thermal diffusivity and later calculating thermal conductivity through Equation 3.1, results are shown in Figure 3.11. The test was run from RT to 500°C. The discontinuous lines represent thermal diffusivity, which for both slag samples, decreased with the increase of temperature. The continuous lines show that thermal conductivity of the samples increased with temperature, with a slower rate after 100°C. For the case of C slag, thermal conductivity fluctuated with the increase of temperature around 1.75 $[W/mK]$. It was concluded that thermal conductivity of both slag samples behaved quasi-constant at 1.7 $[W/mK]$, similar to the results obtained by Gil et al. in 2014 [32].

## 3.3 Summary and work proposal

The results found in literature, concerning thermo-physical properties of copper slag and other recycled materials, are summarized in the following tables.

Table 3.6: Resume table of thermo-physical properties of copper slag as storage material.

| Authors | Sample's Id. | Type of sample | $\rho$ $[kg/m^3]$ | Stability | $Cp$ $[J/gK]$ | $k$ $[W/mK]$ |
|---|---|---|---|---|---|---|
| Curto and Stern [35] | slag C&S | not defined | 4300 - 4400 | Thermally and mechanically stable in structure up to 1200°C | 0.670 - 1.004 | not found |
| Navarro et al. [5] | slag P | powder | 3600 | Thermally and chemically stable up to 800°C | 0.571-1.180 | 0.8 |
| | slag B | | 3700 | | 0.650-0.990 | 1.1 |
| Gorai et al. [29] | Slag G | solid | 2800-3800 | not defined | not defined | not defined |

Table 3.6 presents the main properties of copper slag, to consider in this work for its characterization, based on the author of the corresponding study, and the type of sample that was evaluated (solid or powder). It is clear that copper slag thus far, has only been studied enough to have a general view on its properties, in order to consider it as a potential storage material for TES. However, to be able to use it as a filler material in a packed-bed storage design, more data concerning copper slag's properties is required, in a such a way that can be evaluated as a cost-effective alternative for TES systems.

Table 3.7 shows the characterization results of slags from the steel making industry. It is presented as well, the methodology approach for each case, in order to establish the different experimental methods that can be used, to characterize copper slag samples on this work. Must be noted that properties results presented in a range value, like thermal conductivity or specific heat capacity, consist of the results obtained over a range of temperature, from their respective study case. Furthermore, single values represent properties measured on a specific temperature (generally RT).

Table 3.7: Resume table of properties of slags from the steel making industry, with corresponding measurement methodology.

| Authors | Sample's Id. | $\rho$ $[kg/m^3]$ | | $Cp$ $[J/gK]$ | | $k$ $[W/mK]$ | Thermal stability | Chemical stability and characterization |
|---|---|---|---|---|---|---|---|---|
| | | Apparent | Skeletal | DSC method | LFA | LFA + EQ. | TGA (air atmosphere) | SEM & XRD |
| Ortega, Calvet, et al. [4] | Slag 1 | 3430 | - | 0.865 | - | 1.47 | Stable after 3 heating cycles (200ºC to 1000ºC) | Primarily composed of metal oxides. No corrosion. Stable. |
| | Slag 2 | 4110 | - | 0.837 | - | 1.51 | | |
| Ortega, Faik, et al. [3] | EAF Slag 1 | 3430 | 3860 | 0.710-0.920 | 0.950 | 1.65-1.23 | Stable after 3 heating cycles (200ºC to 1100ºC) | New phases. Oxidation of other elements. Stable. |
| | EAF Slag 2 | 3770 | 4030 | 0.690- 0.880 | 0.890 | 1.50-1.73 | | |
| Wang et al. [33] | S slag | 3600 | - | 0.713-0.858 | - | 1.70-1.72 | Stable after 3 heating cycles (100ºC to 1000ºC) | Migration of elements forming new phases. Samples more stable |
| | C slag | 3700 | - | 0.717-0.975 | - | 1.85-1.65 | | |
| Agalit et al. [31] | IF slag | 2583 | - | 0.460-0.710 | - | not defined | Stable after 3 heating cycles (100ºC to 1000ºC) | Composed primarily of oxides Stable |
| Gil et al. [32] | EAF | 3170 | 3510 | 0.650-0.860 | - | 1.70 | Stable up to 1000ºC | - |

Table 3.7 presents the properties and characteristics that need to be taken into account in this work to properly characterize copper slag, as well as the respective experimental methodology, that have been used by all authors. Nevertheless, it is important to acknowledge the results variety from one sample to another, showing the need to obtain a sampling size of results, large enough to obtain reliable data for copper slag's properties, considering as well its heterogeneous characteristics. Therefore, the present work proposes copper slag's characterization based on the following points: thermal stability analysis, specific heat capacity analysis (with increasing temperature), thermal conductivity of different type of samples (powder and solid), and density of a representative sampling.

# Chapter 4

# Equipment for thermal characterization of storage materials

As it was described in the previous chapter, the thermo-physical properties of copper slag that this work focused on analyzing are: density, specific heat capacity, thermal conductivity and thermal stability. The devices and equipment utilized to measure these properties are described in this chapter.

## 4.1 Differential scanning calorimeter

A differential scanning calorimeter or DSC, is a thermal analytical equipment, that allows to monitor the amount of heat required to increase the temperature of a material. The basic technique of differential scanning calorimetry consist into heating an unknown sample, and a reference material whose thermal properties are well known. The heat flow needed to keep the sample and the reference material at the same temperature, is registered as function of temperature or time. The sample can be heated at different heat rates and can be analyzed isothermally. The heat flow curve obtained from the experience can provide information about the sample's properties, like phase transition points, enthalpies of transition, chemical reactions at certain temperature range, or its specific heat capacity. Figure 4.1a shows an example of heat flow curves as a function of temperature obtained by a DSC analysis. In this case, exothermic heat flow is plotted upwards, meaning that results in the positive area are releasing heat. The curve shows a reactive behaviour at certain temperature during its first cycle of heating, which in this case, represents the glass transition temperature of this material.

On Figure 4.1b, another example of a DSC experimental result is presented. In this case the resulted data of the measurement was adjusted with a software specifically for DSC data analysis. This software allows to construct a baseline; which consists on a signal bias inherent in the system, that needs to be subtracted in order to calculate properly the amount of energy participating in the reaction; subsequently, allowing calculation of enthalpies of transition or

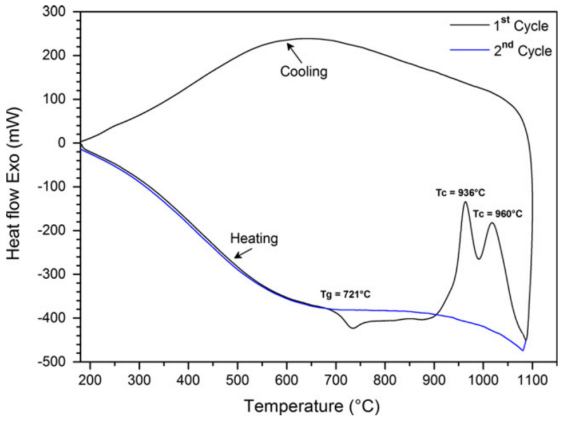


(a) Heat flow curves for heating and cooling [36]

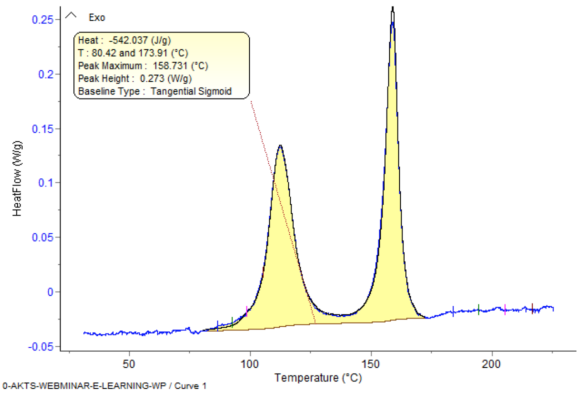


(b) Baseline arrangement through DSC software

Figure 4.1: Example of DSC curve results for different analysis of a material

specific heat capacities as a function of temperature. If an analysis software is not provided, another alternative to adjust the heat flow data, is to run an empty test (no sample or reference material considered), and subtract that information to the actual sample results that is being tested.

The other technique to analyze and measure properties like specific heat capacity, consists of heating at the same rate a sample of the unknown material and a reference material; since they will react differently to the same amount of energy, the temperature difference of the materials can be measured. This technique is known as differential thermal analysis (DTA) and can be used to calculate specific heat capacity of an experimental sample.

The analysis approach of DSC instruments to determine specific heat capacity ($Cp$) of solid materials, can be address as apparent or real specific heat capacity, each term depends on the technique applied to measure the sample (DSC or DTA), and whether or not the data of the reference material is tacked into account when calculating the samples material properties. For instance, if the $Cp$ values are calculated by considering the heat flow data of the run test, the resulting curve corresponds to the apparent $Cp$ of the sample, in the on going temperature range. This curve is calculated through Equation 4.1, where $H$ is the heat flow $[W]$, adjusted after creating the baseline, $m$ is the mass $[g]$ of the sample, and $\beta$ is the temperature rate $[K/s]$ defined during the set up of the test.

$$C_p = \frac{H}{m\beta} \qquad \beta = \frac{\Delta T}{t} \tag{4.1}$$

To calculate the real $Cp$ curve through a DSC test, three measurements need to be performed. The first one is the baseline construction by running a test with empty crucibles, that is to say, with no sample or reference material inside the DSC equipment. Then, the reference sample is tested, which specific heat capacity is well defined. Finally the experimental sample is tested. Through the data recorded in every test, the system's signal bias from data can be removed through the baseline created on the first run; while with the data from the second run, and an imported $Cp$ curve of the reference sample (provided by the corresponding software fro the DSC instrument), a ratio of its specific heat can be calculated. Then, a

$Cp$ curve can be obtained of the "unknown" sample, through the ratio method provided by the software. Usually the known material used as reference consists of sapphire. Figure 4.2 shows an example of a $Cp$ curve obtained from the methodology described.

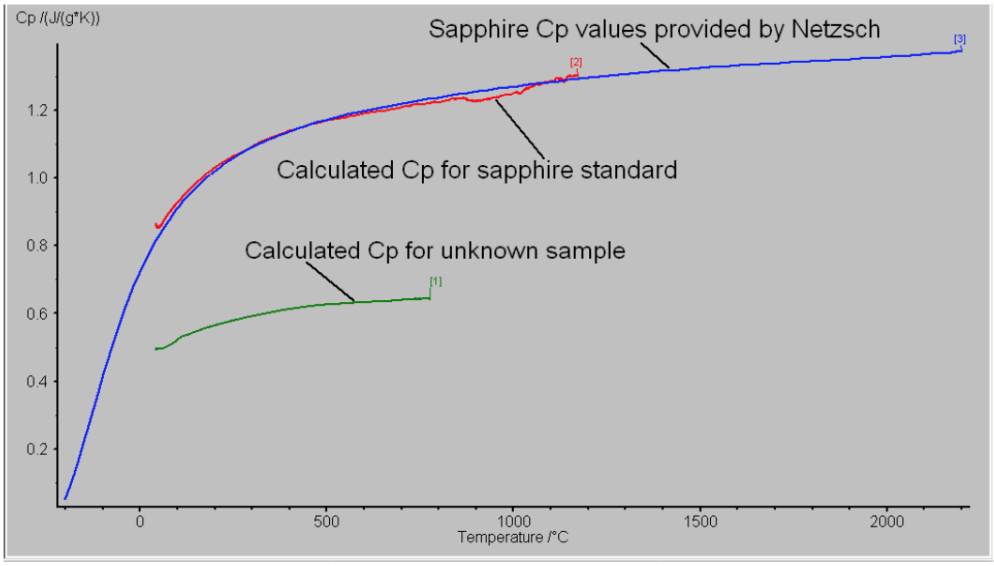


Figure 4.2: Calculated $Cp$ curves for sapphire and "unknown" samples compared with imported sapphire data [37].

## 4.2 Transient line source method

Within the methods to measuring thermal conductivity and other thermo-physical properties of solid materials, one of the most commonly used approaches consist on the use of transient line source (TLS) method, which has been used for over 50 years to measure thermal conductivity of solid, porous materials and soils. The basic technique consists of a needle (probe) with a heater and temperature sensor inside, which is inserted into a sample. A current is passed through the heater, the temperature of the probe is monitored over time, and then analyzed to determine thermal conductivity for the sample. More recently, the heater and temperature sensor have been placed in separate needles. In the dual probe, the analysis of the temperature versus time, yields information on resistivity and heat capacity as well as thermal conductivity.

Thermal properties devices based on TLS method, can be provided with different probes for different sample materials and property analysis. Each probe is relatively large and robust making them easy to use. Heating times are kept as short as possible to minimize the time required for a measurement, but for this same reason, this type of devices require high resolution temperature measurements and special algorithms to measure thermal properties, which are analyzed during a heating and cooling interval.

Figure 4.3 shows a portable device for thermal property analysis called KD2 Pro from Decagon Devices, Inc. This type of device uses different type of needle sensor for measuring properties, and each of them uses an algorithms based on the property to measure, and the

(a) KD2 Pro components (b) SH-1 double needle sensor (c) TR-1 needle sensor

Figure 4.3: KD2 Pro from Decagon Devices Inc. and sensors for properties measurements.

physical characteristics of the needle. These specifications can be found in annex A.

The dual needle SH-1 sensor of Figure 4.3b, allows to measure volumetric heat capacity, thermal resistivity, thermal conductivity, and thermal diffusivity (specific heat capacity can be determine by knowing the sample's density). This sensor is compatible with most solid and granular materials. Figure 4.3c shows TR-1 sensor, which measures thermal conductivity and thermal resistivity. This needle is designed primarily for soil, concrete, and other granular or solid materials, where an appropriate sized hole can be easily drilled, or a pilot pin can be inserted (in the case of uncured concrete).

## 4.3 Thermal gravimetric analysis

Thermal gravimetric analysis or TGA, is a technique in which the mass of a sample material is monitored as a function of temperature or time, as the sample specimen is subjected to a controlled temperature program, in a controlled atmosphere. The sample is placed on a precision balance, and can quantify loss of water, loss of solvents, loss of plasticizer, decomposition, among others possible reactions, like mass gain due to oxidation of the material.

## 4.4 Summary

The equipment and devices described in this chapter, allow the measurement and analysis of thermal properties of materials. DSC and TGA equipment, are able to monitor the material under different thermal conditions, such as high or low temperature range of operation, different heating rates, atmosphere of analysis, or even effects on the sample after a certain number of experimental runs; allowing the determination of temperature points, or amounts of energy, at which the material can be reacting in any sort of way. On the other hand, devices as KD2 Pro are able to measure as well thermal properties, however, on a specific temperature mark, depending on the temperature at which the sample being tested is at. This allows more specific results based on the sample's characteristics solely.

# Chapter 5

# Methodology

In order to determine the thermo-physical properties of copper slag samples, the following methodology was performed.

## 5.1 Sample selection and preparation

The copper slag samples studied in this work come from two different mine sources. They have been tagged EN slag and CO slag based on that. In order to use them for experimental analysis, they were selected and prepared depending on the devices and equipment requirements. The slags were classified depending on four preparation methods.

- **Preparation method A:** Perforated rock samples

  For each slag load, an amount of full size rocks were selected; with a minimum size of 4 to 5 centimeters of width and length, sharp cuts on their sides and with approximately cubic shapes; in order to allow a better grip of the drilling bit and the drilling machine. Rock samples were drilled for two purposes:

  - Collecting slag residue: By drilling the slag rock samples, dust residues were produced, then separated in probes for each perforation. These residues were later used in DSC analysis since small amounts of the material are needed (around the micro-gram scale).

  - Sample for KD2 Pro analysis: Samples used for $Cp$ measurements through KD2 Pro sensors (as described in the previous chapter), need to have two perforations that allow SH-1 double needle sensor to be introduced in the sample rock. Therefore, on the flattest surface of several rock samples, two perforations of 2 to 3 mm of diameter, 30 mm of depth, and separated by a distance of 6 mm, were drilled. A concrete drilling bit was used for this purpose, since they are made for hard surfaces; and in order to avoid the bit to wear off too soon, coolant was applied.

The drilling process was conducted carefully in order to avoid breaking the rock samples. Once the perforations were finished, the samples required to be cleanse, since coolant residue could alter measurements. Therefore, rocks were submerged on ethanol, to rinse off coolant residues. Finally, the rock samples were left to dry at room temperature since ethanol evaporates in these conditions.

- **Preparation method B:** cooked and pulverized

The second type of sample preparation consisted on selecting random amounts of copper slag rocks from each foundry plant (EN slags and CO slags). The samples were thermally treated in an electrical high temperature furnace, heated from room temperature to 800°C, taking approximately 1 hour to reach said temperature. Then, the slags were removed and left to cool naturally for 2 to 3 hours. Once they were cool enough to be grabbed bare handed, the samples were cooked again up to 800°C, and so forth, for 3 full thermal cycles (heating and cooling). Afterwards, the fully cooked slag samples, were taken to the Department of Mining Engineering of University of Chile, to get crushed, pulverized and sieve into 4 sizes of copper slag granulates: a $<$ 0.15 mm; 0.15 mm $<$ b $<$ 0.3 mm; 0.3 mm $<$ c $<$ 0.6 mm; 0.6 mm $<$ d $<$ 1.18 mm. Each final copper slag sample was tagged depending on the foundry plant (EN slag or slag CO) and the size of the granular sample (a, b, c and d), resulting in 16 samples of copper slag granulates. It is important to highlight, that the selected full size rocks were crushed and pulverized all together (only separated based on the foundry plant), with the objective to obtain a more representative sampling for measurements.

- **Preparation method C:** crushed and cooked
A random quantity of rock samples was crushed and then sieved. Afterwards, they were thermally treated by placing them in a crucible, and then cooked 3 times from RT to 800°C on a electrical furnace.

## 5.2 TGA and DSC

Thermal gravimetric analysis and differential scanning calorimetry analysis instruments have similar preparation methods. Both of these instruments need only small amounts of sample of the material to be analysed, as dust or pulverized sample, which is weighted on a precision scale. TGA equipment used for analysis was run by the corresponding technician of the Laboratory of Spectroscopy and Thermal Analysis (LSTA) of DIQBM of University of Chile. On the other hand, DSC tests were run in two different equipment, the first one in the LSTA and the second one in the materials study laboratory of DIMEC USACH. Both DSC and TGA equipment used in the LSTA are from TA Intruments, and can run tests up to 600°C and 800°C, respectively (see Figure 5.1a and Figure 5.1b). DSC from USACH consists of a Perkin Elmer instrument, which can run tests up to 450°C (see Figure 5.1c).

(a) TGA equipment from TA Instruments

(b) DSC equipment from TA Instruments

(c) DSC equipment from PerkinElmer

Figure 5.1: Equipment for thermal analysis used in this work

### 5.2.1 TGA configurations

All TGA tests were conducted considering a single configuration: heating from room temperature to 800°C, temperature rate of 10°C/min, and nitrogen as atmosphere. After each heating process the samples were left to cool naturally. The main variables for the tests that were conducted, consisted principally on; the foundry plant source, the preparation method that was used for the sample, and how many times the sample was heated in the TGA analysis. The slags samples were tagged with the letters corresponding to the foundry plants source; the following letter considers whether the sample came from preparation method A, B or C; and the last number describes if the sample was tested through a single heating run or three heating runs.

- EN-A-3
- EN-B-3
- CO-B-3
- EN-C-1

### 5.2.2 DSC configurations

The first DSC tests in this work were conducted in the LSTA, with copper slag samples obtained through the first method of preparation (slag residue from drilling copper slag rocks), 6 samples were considered. Each was weighted and encapsulated on platinum pans, which then were placed inside the DSC instrument, one measurement at a time. The heating rate for all tests was 10°C/min, and the gas atmosphere was argon and nitrogen. The first in order to obtain results in a the most none-reactive atmosphere, and the later to obtain results closer to the behaviour when using air as HTF. The tests were classified based on the type of purged gas considered, as well as the temperature range over which the test was conducted, and the foundry plant source of the slags.

- EN slag samples under argon atmosphere: On a first instance, a preliminary analysis

of copper slag behaviour with increasing temperature was conducted, by heating the sample from room temperature (RT) to 400°C, and left to cool naturally. Then, the same sample was heated again up to 600°C. Additionally a different slag sample was tested only through a single heating run from RT to 600°C.

- EN slag sample under N2: This sample was heated tested twice under the same temperature range, from RT to 500°C.
- CO slag sample under argon and N2: 4 CO slag samples were tested under argon and N2 atmosphere, 2 samples for each type of atmosphere. The tests were run from RT to 550°C

The heat flow curves resulting from these tests were adjusted through the corresponding software from TA instruments, in order to calculate $Cp$ curves for each sample, with the baseline already subtracted. Finally a last DSC analysis was conducted through DSC equipment from USACH. The test was run on a EN slag sample (prepared through method C), from RT to 450°C, with a heating rate of 10°C/min, and Nitrogen as atmosphere. In this procedure, two isothermal measurement were added during the begging and at the end of the temperature range (30°C and 450°C, respectively), for 5 minutes. Additionally, the cooling process of the sample was also monitored; analogous to the heating process, with regard to the temperature rate and the time held on upper and lower temperature limits. Furthermore, an empty pan run test was conducted in order to create the baseline, that was later on subtracted to the heat flow results from the sample's test. The heat flow difference obtained was used to calculate a $Cp$ curve, based on Equation 4.1.

## 5.3 KD2 Pro

The KD2 Pro device was furnished by CEGA from the Geology department of University of Chile. This device can measure thermo-physical properties of solid materials, soils and liquids. The sample to be tested needs to reach certain requirements (specially in size), in order to obtain a reliable result. To measure thermal conductivity of a solid material, the sample needs to be large enough to allow the TR-1 needle to enter completely, with enough radio of material around it (2 cm minimum). Since copper slag did not present the size enough for this purpose, a different approah was taken. Since the KD2 Pro can also measure properties of soil and granulates, copper slag rocks were crushed and pulverized, hence samples from the method of preparation B were used. In the case for specific heat capacity measurements; which were conducted through SH-1 double needle, due to their smaller length and diameter compared to TR-1 needle; full size copper slag samples were used, since they had the sufficient volume and shapes for this type of analysis.

### 5.3.1 Measurements using TR-1 sensor

It is important to point out that the results of thermal conductivity in a granulated material, are not the same as if the material was measured as a compacted rock, since air between the samples particles affects on the measurement. It is with this perspective, that

it was considered to measure an amount of test tubes of 4 sizes of granulated copper slag (from the second method of preparation), hence, varying the amount of air between particles. Moreover, each sample was measured 4-5 times, with different densities inside the same test tube. The density of the sample was changed by compacting the amount of mass of the material inside the test tube. That is to say, knowing the tube's volume, and changing the amount of mass of the slag sample inside of it, the density of the copper slag test sample was changed. Thus, with a more compacted sample, thermal conductivity results increases as well as the reliability of the results, since the amount of air between particles of slag is being decreased. Basically the samples porosity is being diminished.

By considering the measurements for each density of the test tube sample and the different size of the granulates, an amount of 16 measurements were conducted in total. The test tubes used for this analysis, were made of PVC since its low thermal conductivity would not alter the results. Their volume was calculated by measuring the mass of water needed to fill the test tube. The following steps correspond to the methodology for granulated copper slag samples (replicated for the 4 sizes of granulated slag a, b, c and d):

a. A special sacrifice needle, that comes with the KD2 Pro equipment, is inserted in the material in order to create a hole for the actual needle sensor to go through. Since any bending of the needle needs to be avoid, it is important to always use the sacrifice needle, in such a way to test the materials resistance and compactness.

b. The needle is inserted on the material for 5 minutes, to reach thermal balance with the sample.

c. The cable entry of the needle is connected to the KD2 Pro device, which automatically identifies the type of needle that it is being used.

d. The KD2 Pro is configured to measure every 15 minutes (as suggested by the manual), considering 5 minutes of the actual measuring of thermal conductivity, and other 10 minutes to stabilize the sensor.

e. After 6 to 9 measurements (1 to 1.5 hours), the device is paused, and the needle is pulled out. The results are saved automatically on the data base of the device, including thermal resistivity, temperature of the measurement, and the time at which the device started measuring. Once the device is paused, the error related to the measurement is shown on the screen.

f. The test tube is emptied and the mass of copper slag inside is measured.

g. The test tube is then placed under a press, where the same copper slag sample from before is used to fill the test tube again. However, this time compacting small amounts of the sample, one little bit at a time, with the help from the press machine. The manometer of press allows to know the pressure that it is being applied while the small amounts of sample are being added. The first pressure that is used is only up to 20 $[kg/cm^2]$. This methodology allows to control the amount of mass added in order to change the sample's density inside the test tube.

h. Once the test tube is filled with the material, the sacrifice needle is used in order to help the needle sensor to be inserted.

i. Steps b to h, are repeated until 4 different densities of the material inside the test tube are measured.

j. The pressure used to compact the material during the second and third instance of compression, is 40, 60, and up to 80 $[kg/cm^2]$ maximum, since after this value the PVC tube starts to deform itself.

k. Once a total of 4 complete measures are completed, that is to say, for each of the 4 granulated slag sizes.

l. Finally the results are registered on a sheet.

### 5.3.2 Measurements using SH-1 double needle sensor

The SH-1 double needle sensor, as it is described in chapter 4, it is used for measuring specific heat capacity on a constant volume. The samples that were used for measuring this property, were prepared through the first method, therefore, they have been already drilled and cleanse for measuring.

The following methodology was used for the rock slag samples:

a. The diameter of the perforations is 3 mm, this causes the needles of the sensor to not fit properly inside the wholes. Therefore, in order to avoid air from disrupting the measurements, a silver paste for thermal conductivity is used to cover both needles and fill the wholes completely.

b. Once the sensor is inserted on the rock sample, the KD2 Pro is connected to the entry of the SH-1 needle, and it is configured to measure every 15 minutes.

c. After an hour, the device is paused and the needle is pulled out.

d. The process is repeated for 6 different rock samples.

e. The results that the KD2 Pro returns for thermal resistivity are in $[^oCcm/W]$, therefore, the density of the rock sample needs to be measured in order to calculate the $Cp$.

f. The rock sample is weighted, and its volume is estimated by displacement of water mass on a beaker. This apparent density is used for estimating apparent $Cp$ of the copper slag rock sample.

## 5.4 Density measurements

For density measurement, a simple Archimedes's principle was considered, since is a sufficient approach for a general analysis of this property.

First an amount of 40 samples of copper slag rocks were selected, with different sizes and shapes, from each foundry plant. They rock samples were weighted when dry ($w_{air}$); at room temperature and atmospheric pressure; and then weighted again while submerged on water ($w_{water}$). The density is determine by using Equation 5.1.

$$\rho_{Archimedes} = \left( \frac{w_{water}}{w_{water} - w_{air}} \right) \cdot (\rho_{water} - \rho_{air}) + \rho_{air} \tag{5.1}$$

## 5.5 Summary

The different experimental approaches for each property, relies on the methodology presented in literature for thermal properties characterization, as well as the available resources and conditions for the development of this work.

The methodology described in this chapter allows to assess the main thermo-physical properties of copper slag in relation to its experimental approach. The purpose of conducting different preparation methods and experimental configurations (specially for DSC and TGA results), is to obtain an overview of the thermal performance of copper slag, in order to verify and narrow down the conditions under which the best results are delivered, such as temperature range or method of preparation. Given that thermal capacity dictates the overall storage performance of materials, to assess the specific heat capacity and thermal stability under several tests, is the main objective to state whether if copper slag can be considered as an alternative for high temperature TES. Additionally, by conducting other experimental approaches, the results can be verified; for instance, the use of the KD2 Pro device to determine specific heat capacity at room temperature, besides its purpose of thermal conductivity measurements.

# Chapter 6

# Results and discussion

## 6.1 Copper slag physical observations

The copper slag samples used for test analysis, were prepared depending on the requirements of the experimental equipment. For each preparation method, the following observations regarding copper slag appearance and mechanical behaviour are presented.

### 6.1.1 Drilled rock samples

From the beginning, it was noted that copper slag samples presented heterogeneous characteristics, with areas more glassy than others, and other areas more porous and rocky. Principally copper slag showed opaque dark colors, with small areas with clear minerals and glassy characteristics, like sample from Figure 6.1a. As well, various samples present volcanic characteristics with amorphous zones without crystallization, like sample from Figure 6.1b and Figure 6.1c.

(a) Glassy copper slag (b) Porous copper slag (c) Porous-rocky copper slag

Figure 6.1: Types of copper slag rock samples used in this work

Figure 6.2: Oxidized slag samples with flat sides

The slags that were drilled, were principally samples with the flattest surfaces possible (see Figure 6.2), this way their gripping to the drilling machine could be more safe. It was observed that some samples fractured easily while being drilled, or by just accidentally hitting the worktable once the perforation was finished. Figure 6.3a shows how the rock sample left small plane areas where the fractured occurred, due to the drilling process. Furthermore, a few samples would just fracture by being hit one against the other, and some others would fracture with little strength (see Figure 6.3b). Most of these cases exposed porous and fibrous areas..

(a) Fractured copper slag sample

(b) Copper slag sample with stringy fracture

Figure 6.3: Copper slag samples with fractures and damages while preparing them

### 6.1.2 Samples cooked and pulverized, and vice-versa

Copper slag samples initially had an opaque dark color similar to charcoal, like the rocks from Figure 6.1. When cooked up to 800°C, the rock samples kept their solid state as it was expected, since the fusion point of copper slag is close to 1300°C. Once the heating was finished, the rocks showed an intense incandescence (see Figure 6.4a). After cooling, the copper slag surface color changed, like can be seen in Figure 6.4b and Figure 6.4c, which is likely to have happened due to oxidation of the surface. After the third heating cycle, the samples did not show any important variation in appearance. When the samples were crushed and pulverized, the color of the samples seemed similar to the original dark color.

(a) Copper slag at 800°C inside the furnace

(b) Small copper slags cooled after cooked

(c) Large copper slags cooled after cooked

Figure 6.4: Copper slag samples when cooked up to 800°C, and after cooling.

When the process was done the other way around, by first crushing the copper slag rocks into granulated samples and then thermally treated 3 times; the copper slag sample showed the same purple-ish color than the previous cases. However, since the granulates were placed and cooked in a crucible for metal melting, only the material closer to the surface changed its color, the granulates from the bottom of the crucible didn't show visible changes. This probably happened since the granulates near the surface are in more contact with air, and therefore oxidation.

## 6.2 TGA results analysis

The TGA results for slag sample EN-A-3 are presented in Figure 6.5. During the first heating run, it can be noticed that a minor mass loss happened over 100 to 300°C, likely caused by water evaporation. Over 300°C, the sample's mass started to increased, with a final mass gain of 4.3%, at the end of the 800°C. This mass increase with temperature, is similar to the TGA results by Ortega et al. [3] and Wang et al. [33], as presented in literature. Therefore, it is likely this mass gain is caused by oxidation in the surface of the slag sample, as it was stated in their analysis.

As for the second and third heating runs, the sample's mass gain decreased considerably,

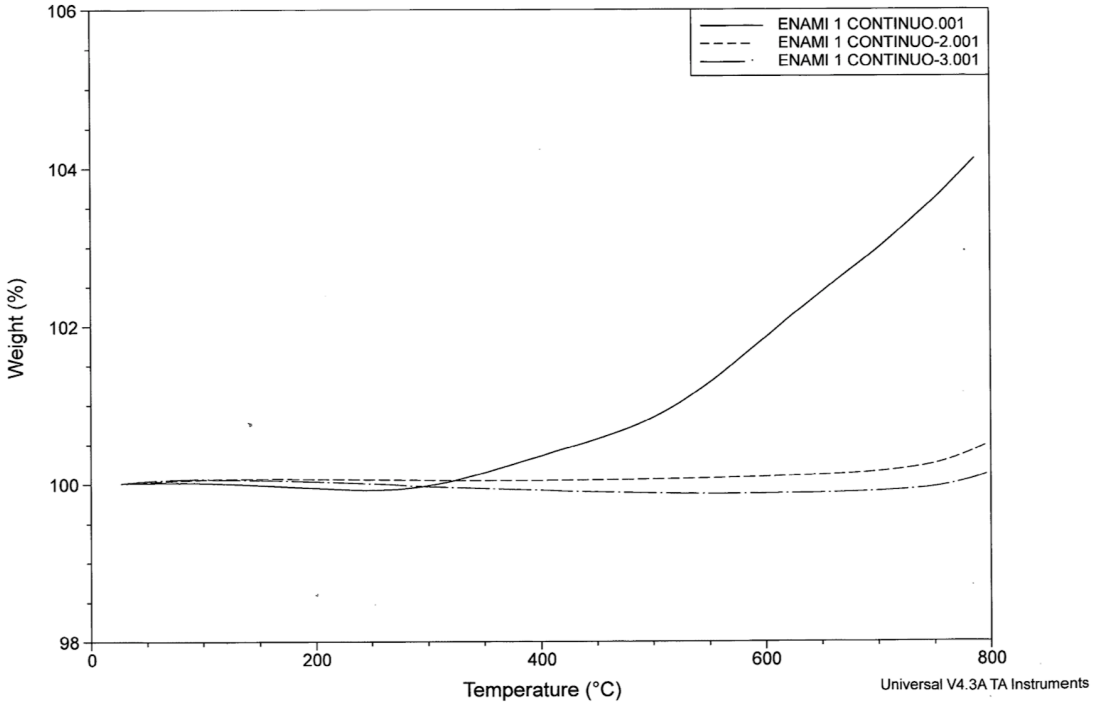


Figure 6.5: TGA results of sample EN-A-3

being almost constant up to 700°C, and with a final mass gain less than 0.5%. This means that no further oxidation is happening, nor any other relevant chemical reactions that can involve mass variation. Henceforth, the sample has been thermally stabilized. Additionally, it is important to notice that the results from Figure 6.5 showed two different mass gain rates during the first heating run; one in the temperature range of 250 to 500°C, and the other with a higher slope from 500 to 800°C.

In order to verify if the samples, after being cooked three times in a furnace, would as well present thermal stability, a single heating run analysis was conducted to sample EN-C-1. The results are presented in Figure 6.6. The sample shows a constant behaviour at the beginning of the test, except for a sudden pick between 100 and 200°C. However, the sample returned to its initial weight and kept stable up to 500°C. The final mass gain was 0.6% at the end of the 800°C.

In contrast with the initial mass gain of the first heating run in Figure 6.5, it is clear that sample EN-C-1 was already oxidized due to its previous thermal treatment. Moreover, if compared with the final mass gain of sample EN-A-3, they are similar, as well as the temperature point at which the mass started to increase. This temperature points were approximately 550°C for sample EN-C-1, and 600°C for sample EN-A-3. Taking into account, that sample EN-A-3 was cooked under a controlled argon atmosphere, in contrast with sample EN-C-1 that was cooked under air atmosphere in an electrical furnace, it can be stated that latter was sufficiently stabilized through this process. On another note, Figure 6.8 shows that the third heating run starts already near the 0.4% of mass gain, this is likely due to an error during the measurement. However, the behaviour is stable and the mass difference from the continuous part to the maximum point in the curve is about 0.5% of mass gain.

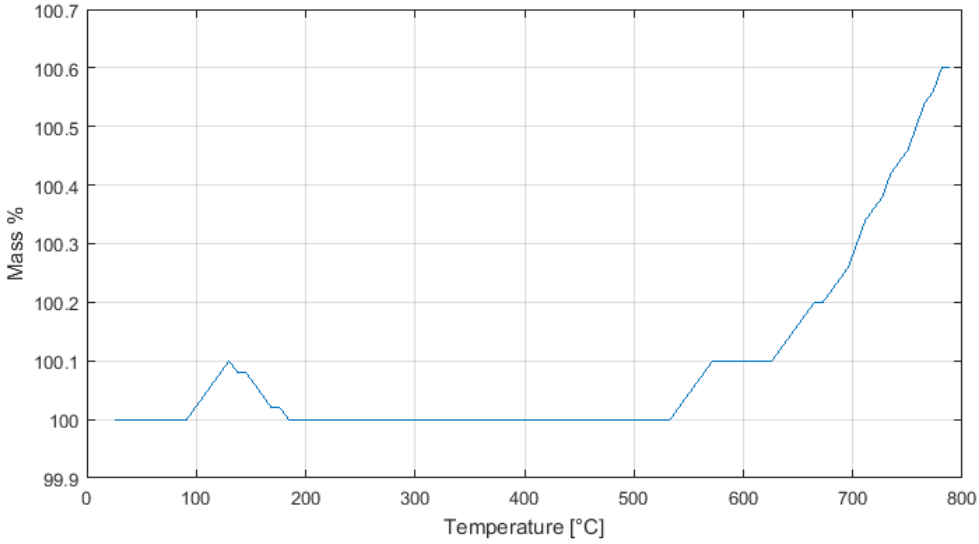


Figure 6.6: TGA results of sample EN-C-1

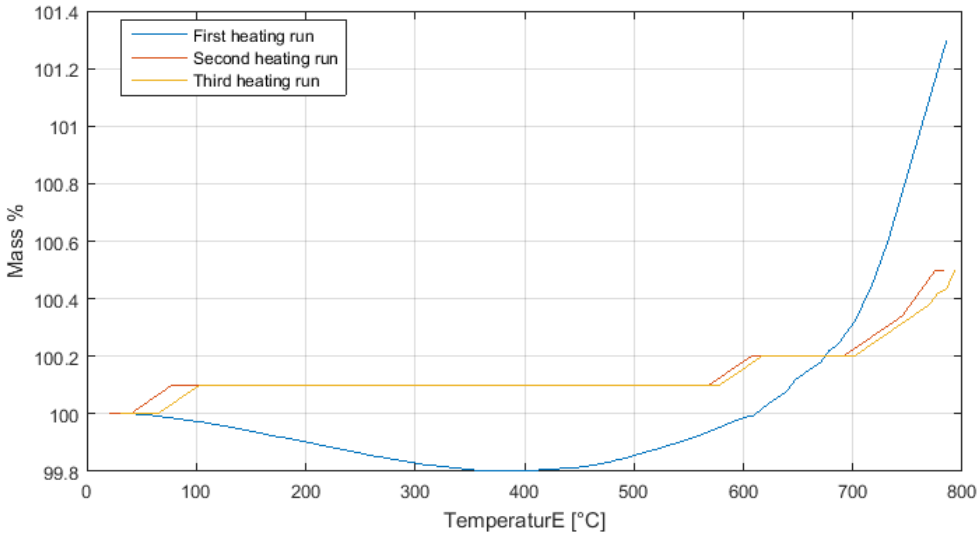


Figure 6.7: TGA results of EN-B-3 sample

Since the method of preparation of sample EN-C-1 consisted on being first pulverized and then cooked, it was likely for it to be thermally stable, as it has been verified with the previous result. When the preparation method was the other way around, that is to say, cooked three times first and the pulverized, as it is the case for sample EN-B-3 and CO-B-3, the following results were obtained (see Figure 6.7 and Figure 6.8). In both cases, a mass loss is noticeable at the beginning of the heating processes. For sample EN-B-3 the mass loss was about 0.2%, however, over 400°C the mass percentage started to increase, about 1.3% from the initial weight of the sample, and 1.5% in the overall mass gain. For sample CO-B-3 the mass loss is about 0.25%, then the increase of mass started at 300°C, with a mass gain about 2.4% from the sample's initial weight, and an overall mass gain of 2.45%. In contrast with the overall mass gain of sample EN-A-3 from Figure 6.5, these mass variations are lower, and the point at which the mass starts to increase is further in higher temperatures. This can be

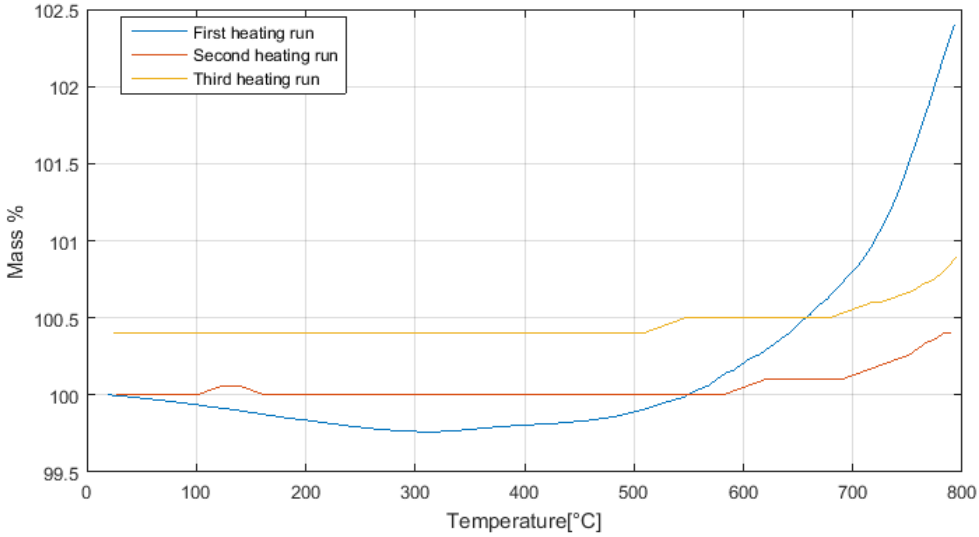


Figure 6.8: TGA results of CO-B-3 sample

interpreted as copper slag being indeed oxidized after the cooking process, however, can not be considered fully stabilized. The final mass gain of both samples at the end of the third run is about 0.5% for sample EN-B-3 and CO-B-3.

Nevertheless, the mass gain percentage of all results are little enough to be considered irrelevant in terms of mass variation.

## 6.3 DSC analysis and $Cp$ curve results

The heat flow results obtained by DSC analysis, were arranged through the TA Instruments software to remove the system signal bias, then through Equation 4.1 the apparent $Cp$ was calculated. As it was described in the methodology chapter, most of the samples that were tested, were not cooked before the test was run, only the sample ran by DSC Perkin was thermally prepared beforehand. Moreover, from this point forward, when referring to $Cp$ results and curves, it assumes the connotation of apparent $Cp$.

Figure 6.9 presents the results for EN slag samples, that were tested under argon atmosphere. On a first instance, the test was ran from room temperature to 400°C (blue curve), showing a stable $Cp$ value around 1.7 $[J/gK]$, which decreased gradually after 200°C. Afterwards, the same sample was run again up to 600°C (red curve), decreasing its stable $Cp$ value to 1.5 $[J/gK]$. However in this case, the curve kept stable for a longer range of temperature. This behaviour, is likely to have happened due to thermal stabilization of the sample, after the first heating run. Subsequently, over 400°C, the sample started to react to temperature, specially at 500°C, where the curve showed a sudden pick.

The last curve from Figure 6.9, is the result of a different EN slag sample. In a shorter temperature range (from 60 to 200°C), the sample showed a stable behaviour, then, the curve

started to decrease, specially near 500°C; where similarly to the previous sample, there is a sudden change in the slope of the curve. Nevertheless, the curve was stable at 1.9 $[J/gK]$ (from 70 to 200°C), and then it decreased to 1.5 $[J/gK]$ near 500°C.

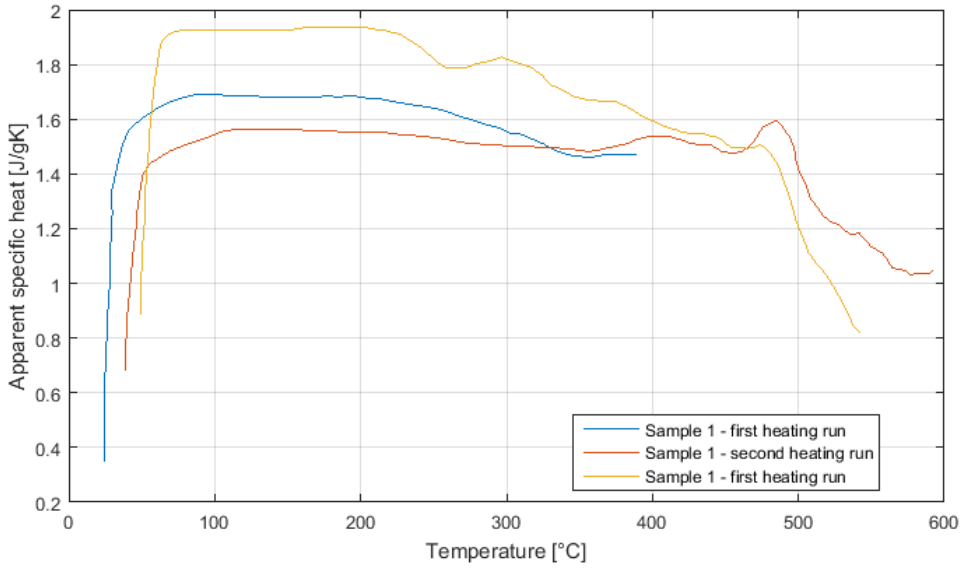


Figure 6.9: Apparent $Cp$ results of EN slag samples measured in argon atmosphere

Additionally, a different EN slag sample was tested in N2 atmosphere. Figure 6.10 shows the results of this sample after 2 heating runs. Both curves did not show any sudden reaction to temperature, except for the gradual decrease of $Cp$. During the first test run, the sample presented high $Cp$ values in the order of magnitude of 1.9 $[J/gK$ to 2.4 $[J/gK]$, through the temperature range from RT to 400°C. Then, during the second heating run, $Cp$ values were reduced to 1.4 $[J/gK]$ to 1.9 $[J/gK]$, in the same temperature range. Such behaviour, of decreased $Cp$ values during the second heating run, happened as well in Figure 6.9.

In contrast, Figure 6.9 showed more stable results than Figure 6.10. It is likely that in the first case, since the sample is being analyzed under argon atmosphere (which is completely inert), the sample is likely to be less reactive at lower temperatures, leaving room to only thermo-physical reactions. On the other hand, nitrogen is likely to be more reactive at higher temperatures, with the different components in the slag. Nonetheless, since N2 is an atmosphere closer to the reality context of a packed-bed, results under this atmosphere are more reliable.

Subsequently, the same DSC tests were run for CO slag samples,in order to compare the results to a different foundry plant. Figure 6.11 shows the results of two different CO slag samples that were analyzed under argon atmosphere. The first sample remained within 1.7 $[J/gK]$ to 2.2 $[J/gK]$, over all the temperature range of the test, in comparison with the second sample, which only kept itself in this range of apparent $Cp$ through 50°C to a little over 300°C. Yet, the latter presented a clear stable behaviour during the first 200°C of the test, while the results of the first sample were more variant. Nonetheless, the first sample did not present abrupt drops of $Cp$ like the second sample, what is more, it had a behaviour and a pick near the 500°C, similar to the red curve from Figure 6.9. Furthermore, the second

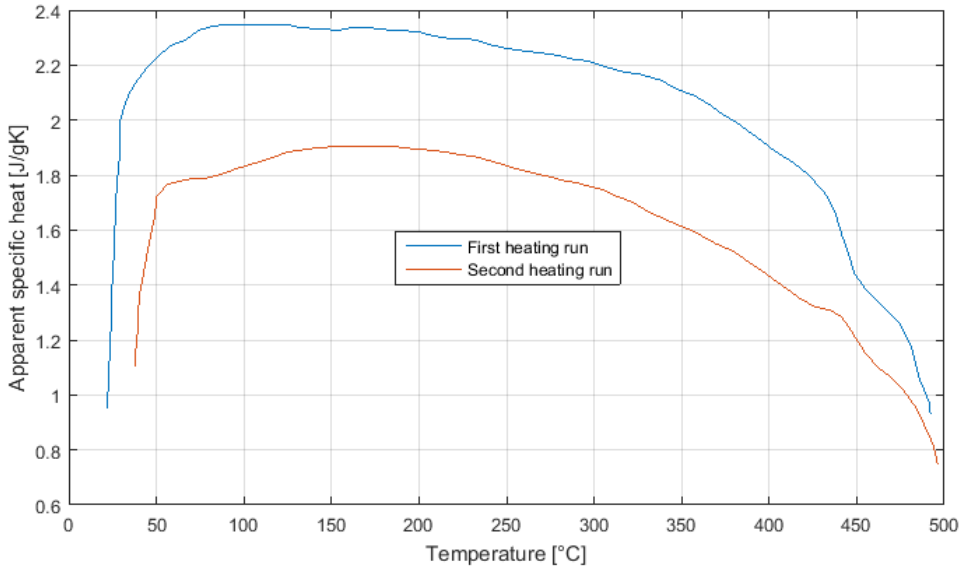


Figure 6.10: Apparent $Cp$ results of EN slag samples measured in Nitrogen atmosphere

sample of this test also presents a change in the slope of the curve, at the temperature points near 200°C and a little under 500°C.

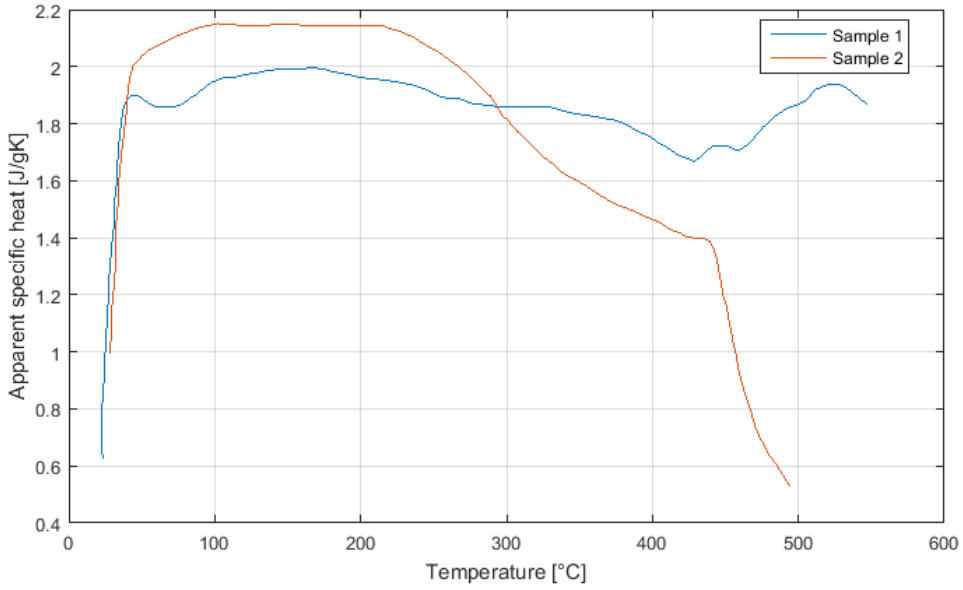


Figure 6.11: Apparent $Cp$ results of CO slag samples measured in argon atmosphere

Figure 6.12 shows the results for two CO slag samples that were tested under N2 atmosphere. The $Cp$ results for sample 1 are constant in 2.0 $[J/gK]$, during the first 200°C of the test; after this point, the curve starts to decrease gradually until reaching the 400°C mark where, it falls abruptly. The second sample, has a smaller range of results between 1.4 $[J/gK]$ to 1.6 $[J/gK]$ during the first 250°C of the test, then the curve gradually decreases. As it has been seen in the previous results, 200°C is the first temperature point at which the apparent $Cp$ curve starts to decrease; the other changes on the slope of the curve (decreasing

on a higher rate), generally occurred over the 450°C temperature mark. What is more, the samples which initial apparent $Cp$ is close to 2.0 $[J/gK]$, tend to have a curve with higher decreasing rates, in contrast with samples with a lower initial value. This leads to that, regardless at which $Cp$ value the curves started, they coincide around 0.6 to 0.8 $[J/gK]$, near the 500°C temperature mark.

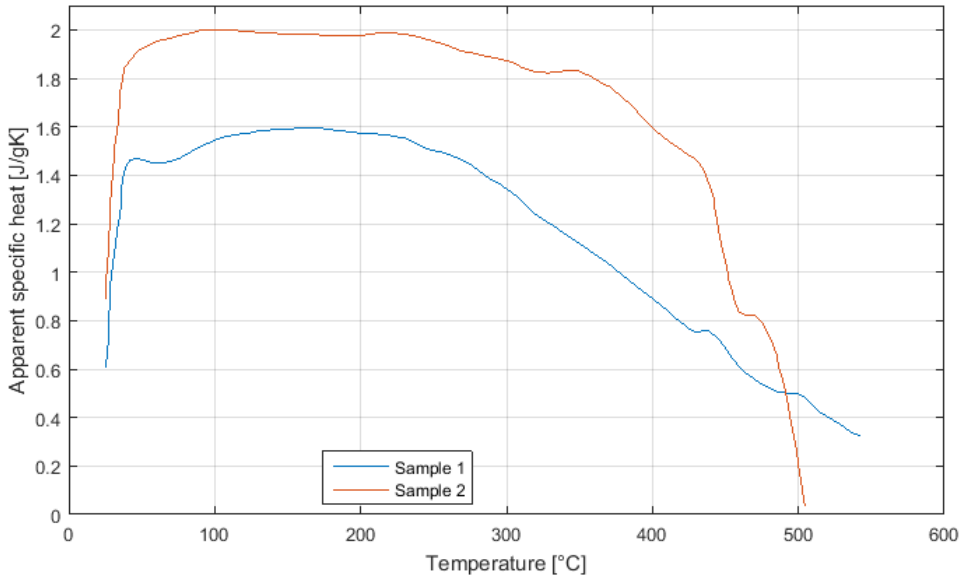


Figure 6.12: Apparent $Cp$ results of CO slag samples measured in Nitrogen atmosphere

The different unstable behaviour of each curve, can not be fully explained with the present information and results. Nevertheless, there are few possible reasons that can be acknowledge based on the correlation of results from TGA and DSC analysis. One of them, is that oxidation is possibly related to variations of the curve. For instance, around the 300°C temperature mark, all the first heating run results from TGA, showed the start of mass gain due to oxidation, which can be somewhat related to the decreasing behaviour of the $Cp$ curve. Other alternative, is that chemical reactions involving the components of the slag, could have being triggered due to the raise of temperature. Furthermore, it is likely that the structure of the copper slag samples is changing; caused by dislocations movement, or even possible glass transition temperatures. However, the analysis regarding chemical composition and structure of the samples, are required to be taken into account to conclude reliably.

Figure 6.13 shows the $Cp$ curve result of an EN slag sample that was previously cooked 3 times in order to thermally stabilize it. The test was conducted through a DSC Perkin equipment with a maximum measuring temperature limit of 450°C. In this case the sample was tested once from RT to 450°C, additionally, the cooling process was as well monitored. In order to subtract the baseline of the equipment, an empty crucible test was conducted, since there was no software available. Then, through 4.1 the apparent $Cp$ curves were obtained. What can be noticed from these results, is that the sample behaved almost linearly from 0.7 $[J/gK]$ at RT, to 1.1 $[J/gK]$ at 450°C, very similar to the DSC results by Ortega et al. [3] and Wang et al. [33], from Figure 3.8 and Figure 3.9, respectively. Furthermore, approximately the same values were obtained during the cooling process. From these results, is possible to state that, by thermally stabilizing the sample (i.e. cooked 3 times up to 800°C), the

instability that was presented in the previous results from the 200°C mark, was almost fully eliminated. Nevertheless, this is the only result under this conditions.

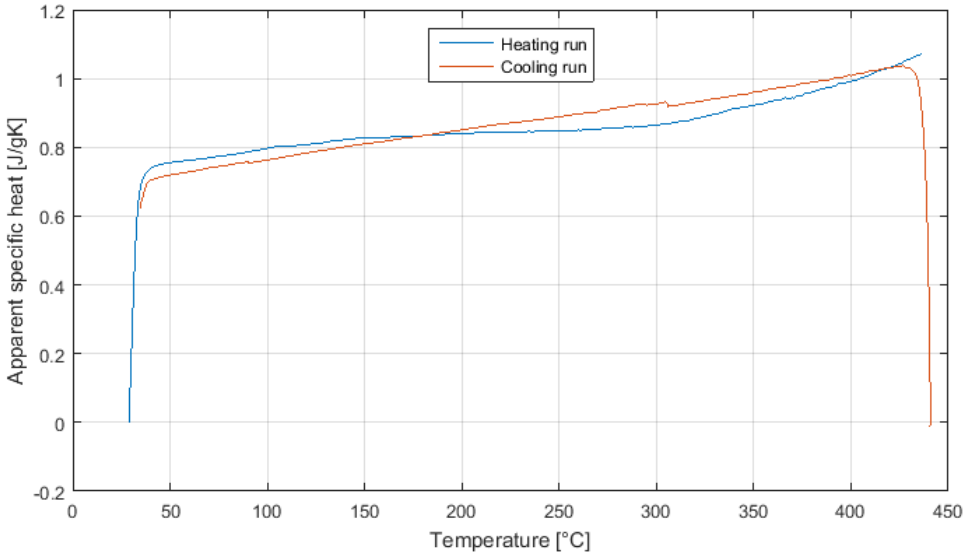


Figure 6.13: $Cp$ curve result of EN slag sample, through a heating cycle (heating and cooling)

The results that were presented before showed two main behaviours; a gradually decreasing curve after the 200°C mark, with a change of slope of the curve near 450°C; and a relatively stable curve with picks over the 500°C mark. The results from Figure 6.13 are under 450°C, and since a number of previous curves (Figure 6.9, Figure 6.11 and Figure 6.12) did not show relevant variation under this temperature limit, is not possible to state that the sample was fully stabilized to higher temperature. Specially since over 450°C, relevant reactions affecting the thermo-physical properties of copper slag take place. Nevertheless, the increasing $Cp$ with temperature is consistent to the analysis found in literature.

The value range of apparent $Cp$ obtained in this analysis is mainly 1.4 to 2.1 $[J/gK]$, for the samples that were not thermally stabilized. These results are higher than conventional solid storage materials (see Table 2.1), and similar to liquid storage alternatives (see Table 2.3). Moreover, these results are higher than the $Cp$ of copper slag found in literature and summarized in Table 3.6, which could be considered highly promising for a storage material alternative. However, the $Cp$ results from Figure 6.13, which have been thermally stabilized, presented results more consistent to the ones obtained by Navarro et al. [5] in Table 3.1. This $Cp$ range, is still considerably higher than EAF slags from literature presented in Table 3.7, and higher than conventional solid storage materials alternatives.

## 6.4 Thermal conductivity and density

Figure 6.14 shows the results of thermal conductivity of the different copper slag test tubes, versus their relative density. As it was expected, thermal conductivity increased with density, since the change of density is related to the change of porosity inside the test tube;

either caused by the use of smaller granulated samples, or due to a more compressed sample; thus diminishing the amount of air between a particle and another, allowing a better thermal conductivity through the material itself.

However, a rock sample of copper slag, has a higher density than the samples used in this analysis. Therefore, by establishing the density of copper slag, and based on the results distribution from Figure 6.14, thermal conductivity of a rock sample can be assessed. Nevertheless, the quantity of slag test tubes required for this purpose needs to be large enough to be a reliable statistical sample, at least over a number of 20. The results of Figure 6.14 only considers 16 test tubes per foundry source of the copper slag, mainly due to low resistance to deformation of the test tube after a pressure limit. Therefore, more thermal conductivity tests require to be performed, by adding test tubes with higher densities of compressed slag sample, which is possible by changing the test tube to a more resistant material. Thermal conductivity results through this method, allows the assessment of the property, at the temperature at which the sample is. Therefore, an analysis of the effects of temperature on thermal conductivity can not me conducted.

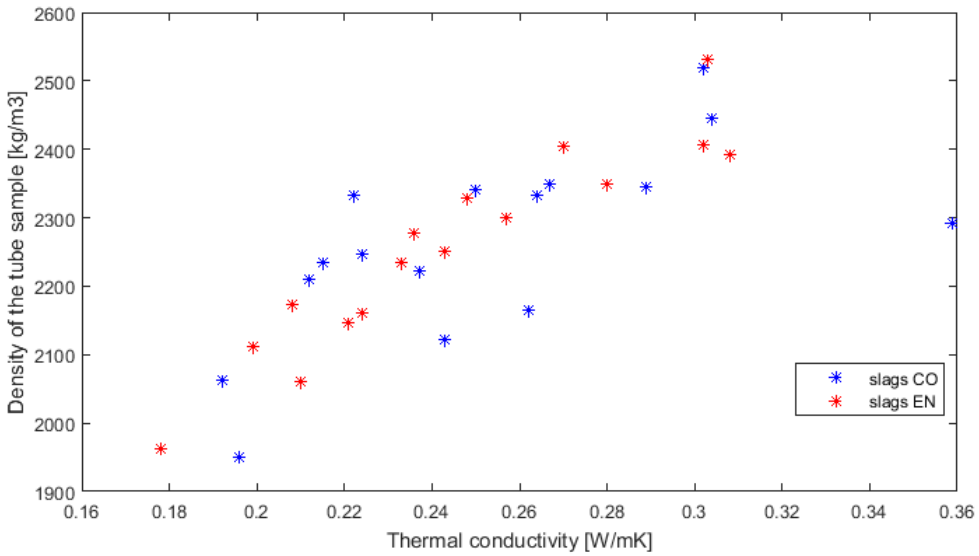


Figure 6.14: Thermal conductivity versus results obtained from KD2 Pro analysis of granulated samples of different sizes and compacted in different densities.

Apparent density of over 40 copper slag samples, from each foundry source, was measured based on the Archimedes's principle (Equation 5.1). The results are shown in Figure 6.15 and Figure 6.16, for EN slag sample and CO slag samples, respectively. The average apparent density for EN slag samples was 3456 $[kg/m^3]$, with a standard deviation of 811 $[kg/m^3]$. For CO slag samples, the average apparent density was 3715 $[kg/m^3]$ and a standard deviation of 606 $[kg/m^3]$. Since copper slag is a highly heterogeneous material, it is foreseeable to have high standard deviation values. Nonetheless, the average density values of these samples, are higher than most of conventional solid storage materials (see Table 2.1), and near the order of magnitude of EAF slags samples from literature (see Table 3.7). Moreover, the average density of copper slag is notably similar to the densities of copper slag, assessed by Navarro et al. [5].

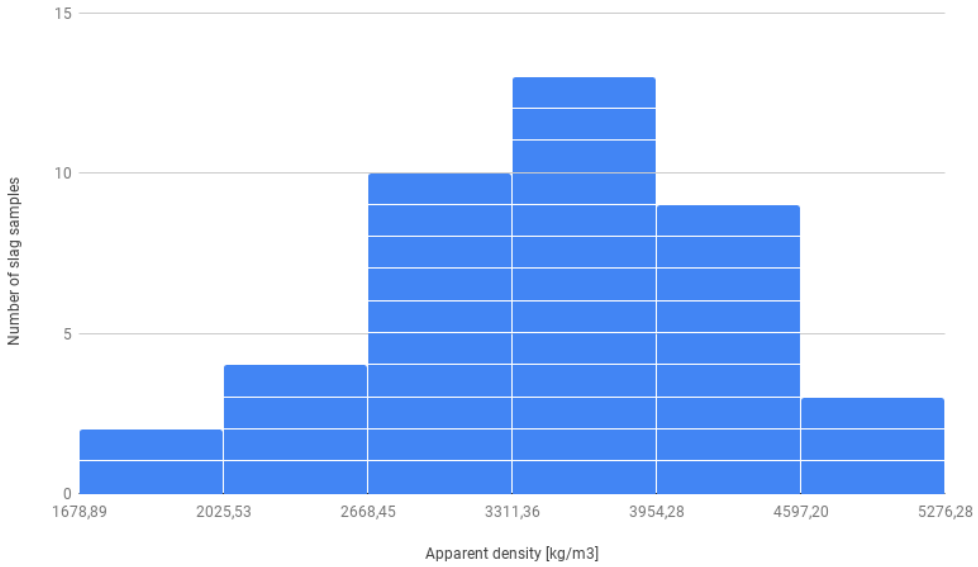


Figure 6.15: Histogram of apparent density results of EN slag samples

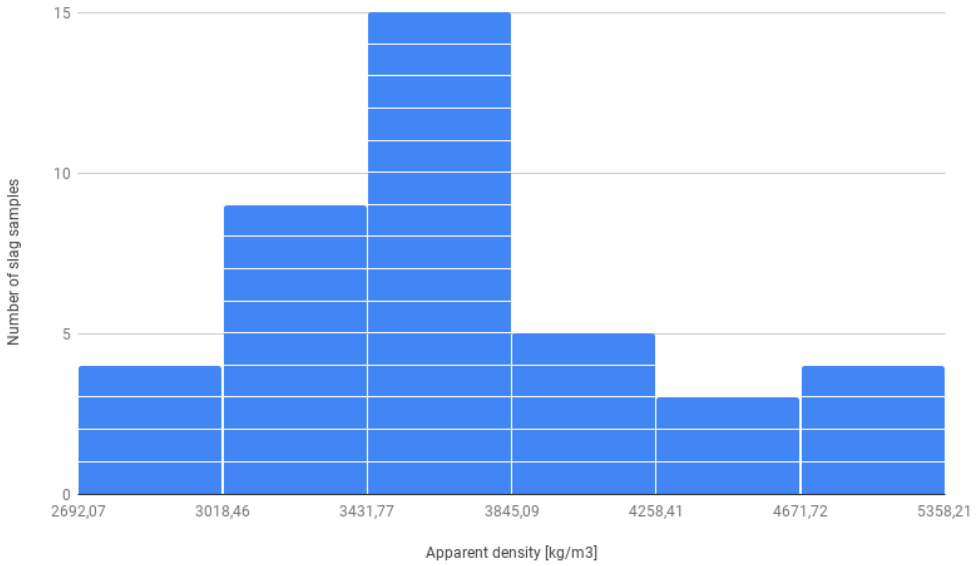


Figure 6.16: Histogram of apparent density results of CO slag samples

Based on the average apparent density results, and the thermal conductivity distribution from Figure 6.14, an estimation of thermal conductivity of a rock sample could be assessed. However, results from Figure 6.14 allow thus far, a first overview of the correlation between porosity of the test tube sample, and its thermal conductivity. Thus, there is not enough information to extrapolate a value for a rock sample by only considering its density.

Ultimately, the properties measured by the SH-1 double needle sensor are presented in Table 6.1. The sensor measured thermal volumetric heat capacity for only 6 copper slag samples. Additionally, specific heat capacity was calculated by measuring the apparent density.

Table 6.1: Results from kd2 Pro analysis using double needle SH-1

| Sample | k $[W/mK]$ | Cv $[mJ/m^3K]$ | apparent $\rho$ $[kg/m^3]$ | Cp $[J/gK]$ |
|---|---|---|---|---|
| A | 2.173 | 5.237 | 3700 | 1.415 |
| B | 1.595 | 2.337 | 3500 | 0.668 |
| C | 1.537 | 2.759 | 3769 | 0.732 |
| D | 2.210 | 3.413 | 3700 | 0.922 |
| E | 1.682 | 2.891 | 3519 | 0.819 |
| F | 1.600 | 4.300 | 3588 | 1.198 |

As it was described in the sensors specifications, SH-1 double needle has a limited range of measurement for different properties, outside this range the accuracy of the measurement decreases. Mainly $Cv$ measurements are the most reliable results when utilizing the SH-1 sensor. The results for $Cp$ considers only the temperature at which the sample is tested, that is to say, room temperature for this case. Comparing this $Cp$ results to the ones assessed through DSC analysis and results from literature, they were very similar and consistent. This means that KD2 Pro device is likely reliable for measuring volumetric heat capacity to estimate specific heat capacity values of a rock sample.

## 6.5 Summary

On a first instance, the appearance and physical properties of copper slag samples were analyzed, showing heterogeneity between different slag samples and on a sample itself. Some slags were more fragile, as well as more dense and heavy than others. A fraction of copper slag samples presented more glassy appearance, while the majority of the samples seemed amorphous and similar to volcanic rocks. Which is likely to happen when copper slag gets cooled down at different rates after the pyrometallurgical process of copper extraction.

The TGA results for thermal stability showed that after cooking the slag samples three times from RT up to 800°C, the final mass gain of all samples was in the order of magnitude of 0.4 to 0.6%. These little mass gains state that, copper slag is almost completely thermally stabilized at the end of the third heating process, likely to the oxidation of the sample's surface during the first heating run. What is more, the preparation method of the slags that allowed thermal stability under fewer heating cycles was preparation method C.

The DSC analysis results for specific heat capacity, presented a variety of curves with behaviours different from one another. However, certain temperature marks were able to point out when the samples had a sudden change in their $Cp$ curve slope, generally, temperatures where the curve decreased on a higher rate. Most of the curves showed a stable behaviour during the first 200°C of the test, after this point, the $Cp$ curves started to decrease. The second temperature point at which the curves changed their slope was near 450 - 500°C. Over this temperature, two curves showed an unexpected pick, which is likely caused by changes in the structure of the copper slag sample, moreover, it is probably related to the fact that copper slag can have more or less a glassy or crystalline structure, which would react differently to higher temperatures.

One of the results (Figure 6.13), involved a slag sample that was thermally stabilized before the test, that is to say, it was cooked three times up to 800°C. This result presented a behaviour consistent to literature, which is a linear curve, from 0.8 to 1.1 $[J/gK]$, over a temperature range from RT to 450°C. The overall $Cp$ values results of the other tests, were considerably higher, from 1.4 to 2.1 $[J/gK]$, however none linearly. This suggest the possibility to thermally stabilized $Cp$ results, in exchange to lower values of the curve; which is still higher than conventional solid storage materials, and the results of EAF slags found in literature. It is important to state that this stabilization can be considered only up to 450°C, since no reliable information at higher temperatures was obtained.

The KD2 Pro results for thermal conductivity showed the direct relation between the granulated sample's density and its thermal conductivity, establishing that by diminishing the porosity of the test tube, a higher thermal conductivity was obtained. However, more results under this conditions need to be conducted, to determine a more reliable correlation, in order to estimate the thermal conductivity of a full size rock of copper slag. On another note, a few thermal conductivity results were obtained with the SH-1 sensor, which are not reliable enough, due to the small amount of results, and the low accuracy of this sensor for this property.

KD2 Pro measured as well volumetric heat capacity that was converted to specific heat capacity, by determining the sample's density. The results were consistent to the values found in literature and to the previous $Cp$ results. This means that KD2 Pro device is likely reliable to measure specific heat capacity for several number of samples, on a specific temperature value, however more measurements need to be conducted in order to validate this.

The slag samples from each foundry plant, presented an average density value of 3456 and 3715 $[kg/m^3]$, and high standard deviations of 811 and 606 $[kg/m^3]$, respectively, which is expected since copper slag is a highly heterogeneous material. These values are consistent to the density results found in literature.

The overall results did not present considerable differences that could be granted to the foundry plant source. What is more, the results present consistency to one another and to the results from literature, validating the results obtained in this work, as such, to state that copper slag presents high thermal capacities due to its high $Cp$ and density results, suggests high energy density for heat storage, at least over the temperature range from RT to 450°C.

# Chapter 7

# Conclusions and future work

The present work, had as objective to characterize copper slag on its thermo-physical properties, with the motivation to use it as a sensible heat material for high temperature TES. As such, the literature review for this study concerned two main issues: thermal properties of copper slag in former studies, and industrial by-products characterization with their respective experimental approach. Based on the these reviews, the thermo-physical properties assessed in this work were, thermal stability, specific heat capacity, thermal conductivity and apparent density.

Regarding $Cp$ results from DSC analysis, it was observed a wide range of values and a general instability around high temperatures. Nevertheless, the order of magnitude of the overall results (DSC and KD2 Pro device), were higher than conventional solid storage materials, even similar to some liquid materials and solar salts. Thus, in addition to its high average density, copper slag can be declare as a high thermal capacity material, specifically over a temperature range from RT to 450°C. Moreover, since copper slag was thermally stabilized, and subsequently a linear $Cp$ curve was obtained, it is possible to place this material as a potential sensible heat storage alternative, specially in contrast with molten salts, which are the main storage media used in TES for CSP. However, the initial interest for the characterization of copper slag relied on the possibility of using it on an higher temperature range than the current one for molten salts, that is to say, copper slag required to perform over the 600°C mark, without jeopardizing its thermal capacity and performance. Yet, this milestone analysis was not approached due to measurement equipment limitations.

From the TGA results, it was possible to validate the thermal stability of copper slags at high temperatures at least up to 800°C (possibly over 1000°C), which presents an advantage for CSP technologies designs regarding the high flexibility of operating temperature. Nonetheless, chemical stability is still a variable that needs to be approached in more detail, specially around corrosion effects of copper slag on the overall pipe and accumulator materials, throughout several heating cycles. Although TGA results implies copper slag's resistance to degradation, is not a feasible indicator of other thermal properties performance to high temperatures, nor corrosive effects. TGA and DSC results suggest that copper slag can, at the very least, be used instead of molten salts on the same temperature range, avoiding risk of freezing or decomposition points, as well as cost reductions due to the usage of a single

tank (instead of the conventional two tank storage for molten salts) and being a lower cost alternative on its own.

The different thermal conductivity results obtained, whether as granulates or full size copper slag samples, presented competitive and consistent values to other storage materials; higher than the liquids alternatives, however with not enough information to state that they are lower than other solids. Although, these results do not give a definitive value of thermal conductivity, it does present a view on the effect of porosity on the overall thermal conductivity of the medium, which is a parameter that requires to be taken into account in further packed-bed models analysis, for the charging and discharging cycles.

The fact that thermal properties analysis over the 600°C mark, were not conducted on this work due to equipment limitations; an opportunity to deepen copper slag's characterization over higher temperature range is presented. This is some of the analysis that require to be performed on a future stage of the characterization study of copper slag. Moreover, since the $Cp$ curves in this work showed two particular types of behaviour, which are thought to be related to the material's structure (glassy or crystalline), it is suitable to consider as well, further tests through XRD and SEM for structure analysis.

As an overall conclusion, the results obtained in this work allowed a first approach on copper slag characterization for its use in packed-bed configuration TES. It was able to state that copper slag has high thermal capacity in contrast with conventional alternatives, and other industrial by-products that have been studied and validated in packed-bed models. Therefore, this work settles the ground floor for further studies on copper slag characterization, on a higher temperature range context, to be implemented in high temperatures TES, with the purpose to be used in high power generation CSP technologies, and exploit the solar resource.

## 7.1 Future work

A larger amount of thermal conductivity results must be conducted on more compressed samples, until determine a reliable sampling to estimate thermal conductivity of a full size sample. Moreover, since the interest in copper slag is to be used in high temperature TES, $Cp$ and thermal conductivity analysis over 600°C, are the main thermal properties to consider on future experimental approaches to complement the results obtained in this work.

As it was first sentenced on the results, copper slag is likely to present reactions at higher temperatures, which in order to determine the reasons behind these possible reactions, is by conducting XRD and SEM analysis, for composition and structure of copper slag at certain temperature points and over a high temperature range.

As for the performance of copper slag under several heating cycles, a chemical stability analysis is required, as well to toxicity and corrosive analysis, by leaving copper slag sample under high temperatures for several hours, and then compare its chemical composition before and after the cooking process.

# Bibliography


[1] Jose Manuel Valverde, Juan Miranda-Pizarro, Antonio Perejón, Pedro E. Sánchez-Jiménez, and Luis A. Pérez-Maqueda. Calcium-Looping performance of steel and blast furnace slags for thermochemical energy storage in concentrated solar power plants. *Journal of CO2 Utilization*, 22(July):143–154, 2017.

[2] M. Romero and J. González-Aguilar. Next generation of liquid metal and other high-performance receiver designs for concentrating solar thermal (CST) central tower systems. *Advances in Concentrating Solar Thermal Research and Technology*, pages 129–154, 1 2017.

[3] Iñigo Ortega-Fernández, Nicolas Calvet, Antoni Gil, Javier Rodríguez-Aseguinolaza, Abdessamad Faik, and Bruno D'Aguanno. Thermophysical characterization of a by-product from the steel industry to be used as a sustainable and low-cost thermal energy storage material. *Energy*, 89:601–609, 2015.

[4] I. Ortega, A. Faik, A. Gil, J. Rodríguez-Aseguinolaza, and B. D'Aguanno. Thermophysical Properties of a Steel-making by-product to be used as Thermal Energy Storage Material in a Packed-bed System. In *Energy Procedia*, volume 69, pages 968–977. Elsevier B.V., 2015.

[5] M. E. Navarro, M. Martínez, A. Gil, A. I. Fernández, L. F. Cabeza, R. Olives, and X. Py. Selection and characterization of recycled materials for sensible thermal energy storage. *Solar Energy Materials and Solar Cells*, 107:131–135, 2012.

[6] IEA. 2018 World Energy Outlook - Executive Summary. *Oecd/Iea*, page 11, 2018.

[7] S.Ashok. Solar energy, 2019.

[8] K. Lovegrove and W. Stein Csiro. Introduction to concentrating solar power (CSP) technology. *Concentrating Solar Power Technology: Principles, Developments and Applications*, pages 3–15, 2012.

[9] Antoni Gil, Marc Medrano, Ingrid Martorell, Ana Lázaro, Pablo Dolado, Belén Zalba, and Luisa F. Cabeza. State of the art on high temperature thermal energy storage for power generation. Part 1-Concepts, materials and modellization, 2010.

[10] D. Kearney, B. Kelly, U. Herrmann, R. Cable, J. Pacheco, R. Mahoney, H. Price,

D. Blake, P. Nava, and N. Potrovitza. Engineering aspects of a molten salt heat transfer fluid in a trough solar field. *Energy*, 29(5-6):861–870, 4 2004.

[11] Ming Liu, N. H. Steven Tay, Stuart Bell, Martin Belusko, Rhys Jacob, Geoffrey Will, Wasim Saman, and Frank Bruno. Review on concentrating solar power plants and new developments in high temperature thermal energy storage technologies. *Renewable and Sustainable Energy Reviews*, 53:1411–1432, 2016.

[12] Doug Brosseau, John W Kelton, Daniel Ray, Mike Edgar, Kye Chisman, and Blaine Emms. Testing of Thermocline Filler Materials and Molten-Salt Heat Transfer Fluids for Thermal Energy Storage Systems in Parabolic Trough Power Plants . *Journal of Solar Energy Engineering*, 127(1):109–116, 2 2005.

[13] Luc Moens and Daniel M. Blake. Advanced heat transfer and thermal storage fluids. *International Solar Energy Conference*, pages 791–793, 2005.

[14] E. Flores. A Review of Latent Heat Thermal Energy Storage for Concentrated Solar Plants onthe Grid. *The Journal of Undergraduate Research at the University of Illinois at Chicago*, 8(1), 2015.

[15] H. Grirate, H. Agalit, N. Zari, A. Elmchaouri, S. Molina, and R. Couturier. Experimental and numerical investigation of potential filler materials for thermal oil thermocline storage. *Solar Energy*, 131:260–274, 6 2016.

[16] HUGH REILLY and Gregory Kolb. An Evaluation of Molten-Salt Power Towers Including Results of the Solar Two Project. 2001.

[17] Ulf Herrmann, Michael Geyer, and Dave Kearney. Overview on Thermal Storage Systems. *FLABEG Solar International GmbH February 20 - 21, 2002 Workshop on Thermal Storage for Trough Power Systems*, page 23, 2002.

[18] Rainer Tamme. Thermal Energy Storage for Industrial Process Heat and Power Generation. 2011.

[19] Martin Forster. Theoretical investigation of the system SnOx/Sn for the thermochemical storage of solar energy. *Energy*, 29(5-6):789–799, 4 2004.

[20] Luc Moens, Daniel M. Blake, Daniel L. Rudnicki, and Mary Jane Hale. Advanced thermal storage fluids for solar parabolic trough systems. *Journal of Solar Energy Engineering, Transactions of the ASME*, 125(1):112–116, 1 2003.

[21] H Mehling and L F Cabeza. *Heat and cold storage with PCM*. 2008.

[22] L.F. Cabeza, A. Castell, C. Barreneche, A. de Gracia, and A.I. Fernández. Materials used as PCM in thermal energy storage in buildings: A review. *Renewable and Sustainable Energy Reviews*, 15(3):1675–1695, 4 2011.

[23] K S do Couto Aktay, R Tamme, and H Müller-Steinhagen. Thermal Conductivity of High-Temperature Multicomponent Materials with Phase Change. *International Journal*

*of Thermophysics*, 29(2):678–692, 2008.

[24] Lovegrove, K., Kreetz, H., and Luzzi, A. The first ammonia based solar thermochemical energy storage demonstration. *J. Phys. IV France*, 09:3–581, 1999.

[25] W. D. Steinmann. *Thermal energy storage systems for concentrating solar power (CSP) technology*. Woodhead Publishing Limited, 2014.

[26] 3Rd Miami International Conference 3Rd Miami International Conference. Number December, 1980.

[27] Aamir Shams. *A Study on Effective Thermal Conductivity of Copper Slag Particle Filled Epoxy Composites*. PhD thesis, National Institute of Technology Rourkela, 2013.

[28] Sandhyarani Biswas, Amar Patnaik, and Ritesh Kaundal. Effect of Red Mud and Copper Slag Particles on Physical and Mechanical Properties of Bamboo-Fiber-Reinforced Epoxy Composites. *Advances in Mechanical Engineering*, 4:141248, 2012.

[29] Bipra Gorai, R K Jana, and Premchand. Characteristics and utilisation of copper slag—a review. *Resources, Conservation and Recycling*, 39(4):299–313, 2003.

[30] Guillermo Ugarte. Metalurgia Extractiva. Pirometalurgia del Cobre, 2018.

[31] H. Agalit, N. Zari, and M. Maaroufi. Thermophysical and chemical characterization of induction furnace slags for high temperature thermal energy storage in solar tower plants. *Solar Energy Materials and Solar Cells*, 172(May):168–176, 2017.

[32] Antoni Gil, Nicolas Calvet, Iñigo Ortega, Elena Risueño, Abdessamad Faik, and Javier Rodríguez-aseguinolaza. Characterization of a by-product from steel industry applied to thermal energy storage in Concentrated Solar Power. *Eurotherm Seminar #99 Advances in Thermal Energy Storage*, pages 1–9, 2014.

[33] Yizhu Wang, Yang Wang, Heping Li, Junhu Zhou, and Kefa Cen. Thermal properties and friction behaviors of slag as energy storage material in concentrate solar power plants. *Solar Energy Materials and Solar Cells*, 182(March):21–29, 2018.

[34] Koki Nishioka, Takayuki Maeda, and Masakata Shimizu. Application of Square-wave Pulse Heat Method to Thermal Properties Measurement of CaO–SiO<sub>2</sub>–Al<sub>2</sub>O<sub>3</sub> System Fluxes. *ISIJ International*, 46(3):427–433, 2006.

[35] Paul Allen Curto, George Stern, and Inc. Gibbs & Hill. 3rd Miami international conference on alternative energy sources. In *High temperature thermal storage using slag*, pages 109–111, 1980.

[36] A. Faik, S. Guillot, J. Lambert, E. Véron, S. Ory, C. Bessada, P. Echegut, and X. Py. Thermal storage material from inertized wastes: Evolution of structural and radiative properties with temperature. *Solar Energy*, 86(1):139–146, 2012.

[37] J E Daw. Measurement of Specific Heat Capacity Using Differential Scanning Calorimeter. *Idaho National Laboratory*, (November):24, 2008.

# Annex A

# KD2 Pro Theory from Operator's Manual

Researchers have used transient line heat source methods to measure thermal conductivity of porous materials for over 50 years. Typically a probe for this measurement consists of a needle with a heater and temperature sensor inside. A current passes through the heater and the system monitors the temperature of the sensor over time. Analysis of the sensor temperature determines thermal conductivity. More recently the heater and temperature sensors have been placed in separate needles. In the dual probe the analysis of the temperature vs time relationship for the separated probes yields information on diffusivity and heat capacity as well as conductivity. An ideal sensor has very small diameter and a length perhaps 100 times its diameter. It would be in intimate contact with the surrounding material and would measure the temperature of the mate- rial during heating and cooling. Ideally, the temperature and com- position of the material in question would not change during the measurement.

Real sensors fall short of these ideals in several ways. A sensor small enough to be ideal would be too fragile for most applications. Measurements in outdoor environments involve changing temperatures; the ambient temperature generally is not constant. Heating moist, unsaturated soil causes water to move away from the heat source, thus altering the water content in the region of measurement, and the hole made for the probe often disturbs the material around it causing a contact resistance between the sensor and the material.

It is a challenge to design a sensor that gives accurate measurements under all conditions. If the sensor is too small it is fragile, and the contact resistance can be high in dry, porous materials. Large sensors require a long heating time, but the long heating time drives water away from the sensor and can cause free convection in liquid samples, thus altering the reading. A high heating rate makes temperature changes easier to read and less susceptible to temperature drift errors, but results in water movement out of the measuring region and free convection in liquids. We recommend long heating times to minimize contact resistance that results in water movement away from the sensor.
Decagon's KD2 Pro design attempts to optimize thermal properties measurements relative to these issues. Our sensors are relatively large and robust making them easy to use. The

KD2 Pro keeps heating times as short as possible to minimize thermally induced water movement and lower the time required for a measurement. We also limit heat input to minimize water movement and free convection. Use of relatively short heating times and low heating rates requires high resolution temperature measurements and special algorithms to measure thermal properties. The KD2 Pro resolves temperature to 0.001 C in temperature. It uses special algorithms to analyze measurements made during a heating and a cooling interval. Algorithms also separate out the effects of the heat pulse from ambient temperature changes. The KD2 Pro uses two different algorithms, one for the dual needle sensor and one for the single needle, based on Carslaw, Jager, and Kluitenberg's line heat source analysis.

## A.1 Dual Needle Algorithm

Heat is applied to the heated needle for a set heating time, $t_h$, and temperature is measured in the monitoring needle, 6 mm distant during heating and during the cooling period following heating. The readings are then processed by subtracting the ambient temperature at time 0, multiplying by $4\pi$ and dividing by the heat per unit length, $q$. The resulting data are fit to the following equations using a nonlinear least squares procedure.

$$T^* = b_0 t + b_1 Ei\left(\frac{b_2}{t}\right) \tag{A.1}$$

$$T^* = b_0 t + b_1 \left\{ Ei\left(\frac{b_2}{t}\right) - Ei\left[\frac{b_2}{t - t_h}\right] \right\} \tag{A.2}$$

Where

$$T^* = \frac{4\pi\left(T - T_0\right)}{q} \tag{A.3}$$

Here, $E_i$ is the exponential integral, and $b_0$, $b_1$ and $b_2$ are the constants to be fit. $T_0$ is the temperature at the start of the measurement and $q$ is the heat input. The first equation applies for the first $t_h$ seconds, while the heat is on. The second equation applies when the heat is off. Compute thermal conductivity from Equation A.4 and diffusivity from Equation A.5.

$$k = \frac{1}{b_1} \tag{A.4}$$

$$D = \frac{r^2}{4b_2} \tag{A.5}$$

You can find the conductivity and diffusivity by fitting Equation A.1 to the transformed data. The correct values of $b_0$, $b_1$ and $b_2$ are the ones which minimize the sum of squares of error between the equations and the measurements. Use the Marquardt (1963) non-linear least squares procedure to find the correct values. This procedure is susceptible to getting stuck in local minima and failing to find a global minimum in some problems (the single needle problem is a perfect example of a bad non-linear least squares problem) but the dual needle problem typically works well. The KD2 Pro can find the three model parameters quickly.

## A.2 Single Needle Algorithm

Heat is applied to a single needle for a time, $t_h$, and temperature is monitored in that needle during heating and for an additional time equal to $t_h$ after heating. Two needle sizes are used; One (the KS- 1) is 1.2 mm diameter and 6 cm long. The other (the TR-1) is 2.4 mm diameter and 10 cm long. The temperature during heating is computed from Equation A.6.

$$T = m_0 + m_2 t + m_3 \ln t \tag{A.6}$$

Where $m_0$ is the ambient temperature during heating (which could include some offset for contact resistance and the heating element being adjacent to the temperature sensor inside the needle), $m_2$ is the rate of background temperature drift, and $m_3$ is the slope of a line relating temperature rise to logarithm of temperature.

Equation A.7 represents the model during cooling.

$$T = m_1 + m_2 t + m_3 \ln \left[ \frac{t}{t - t_h} \right] \tag{A.7}$$

The thermal conductivity is computed from Equation A.8.

$$k = \frac{q}{4\pi m_3} \tag{A.8}$$

Since these equations are long-time approximations to the exponential integral equations (Equation A.1), we use only the final 2 of the 3 data collected (ignore early-time data) during heating and cooling. This approach has several advantages. One is that effects of contact resistance appear mainly in these earlytime data, so by analyzing only the later time data the measurement better represents the thermal conductivity of the sample of interest. Another advantage is that equations 5 and 6 can be solved by linear least squares, giving a solid and definite result. The same data, subjected to a non-linear least squares analysis, can give a wide range of results depending on the starting point of the iteration because the single needle problem is susceptible to getting stuck in local minima. The linear least squares computation is also very fast.

## A.3 The Error (Err) Value

When heat at a constant rate, q is applied to the KD2 Pro needles, the temperature response of the sensor over time can be described by the Equation A.9.

$$\Delta T = -\frac{q}{4\pi k} Ei \left( \frac{-r^2}{4Dt} \right) \tag{A.9}$$

Where $k$ is the thermal conductivity of the medium in which the needle is buried, $D$ is the thermal diffusivity of the medium, $r$ is the distance between the heater and the sensor where temperature is measured, and $E_i$ is the exponential integral. The KD2 Pro uses this

equation to model temperature rise in the dual needle sensor, and uses just the first term of the exponential integral expansion (the logarithm of time) for the single probe sensors. Values of $k$ and $D$ are sought which minimize the difference between model and measured values of temperature rise. Temperature of the needle is measured, so $\Delta T$ is first computed by subtracting the initial temperature from all readings. Temperature rise is further scaled by multiplying by $4\pi$ and dividing by $q$. If we call this new temperature variable $T^*$, then we find the values of $k$ and $D$ that minimize the sum of squares of error.

$$SSE = \sum (T_i^* - M_i^*)^2 \tag{A.10}$$

where the $T_i*$ are the measured values and the $M_i^*$ are values modeled with Equation A.9. Equation A.11 shows the standard error of estimate for the measurements.

$$S_{yx} = \sqrt{\frac{SSE}{n}} \tag{A.11}$$

where $n$ is the number of measurements. The units of $S_{yx}$ are $mC/W$ . It can be made dimensionless if it is multiplied by the thermal conductivity, $k$. This dimensionless value gives the error in fitting the model to data as a value independent of heater current or the thermal conductivity of the medium. The KD2 Pro computes err as in Equation A.12.

$$err = kS_{yx} \tag{A.12}$$

It is a dimensionless measure of the goodness of fit of the model to the data. It can be converted to temperature by dividing by $k$ and multiplying by $q$.

*Note: The Err term is not a rigorous statistical indicator of mea- surement quality, but it serves as a qualitative quality indicator.*

## A.4 Sensor specifications

**10 cm (large) single needle (TR-1)**

Size: 2.4 mm diameter x 10 cm long

Range:
0.1 to 4.0 $\frac{W}{mK}$ (thermal conductivity
25 to 1000 $^oC\frac{cm}{W}$ (thermal resistivity)

Accuracy:
(Conductivity): ±10% from 0.2 to 4.0 $\frac{W}{mK}$
±0.02 $\frac{W}{mK}$ from 0.1 to 0.2 $\frac{W}{mK}$

Cable length: 0.8 m

**3 cm dual-needle (SH-1)**

Size: 1.3 mm diameter x 3 cm long, 6 mm spacing

Range:

0.02 to 2.00 $\frac{W}{mK}$ (thermal conductivity
50 to 5000 $^{o}C\frac{cm}{W}$ (thermal resistivity)
0.1 to 4.0 $\frac{mm^2}{s}$ (diffusivity)
0.5 to 4.0 $\frac{mJ}{m^3K}$ (volumetric specific heat)

Accuracy:

(Conductivity): $\pm 10\%$ from 0.2 to 2 $\frac{W}{mK}$
$\pm 0.01$ $\frac{W}{mK}$ from 0.02 to 0.20 $\frac{W}{mK}$
(Diffusivity) $\pm 10\%$ at conductivities above 0.1 $\frac{W}{mK}$
(Volumetric Specific Heat) $\pm 10\%$ at conductivities above 0.1 $\frac{W}{mK}$

Cable length: 0.8 m